Chapter 12
Elementary Sources and Multipoles

Antoine Chaigne and Jean Kergomard

Abstract Elementary sources, such as monopoles and dipoles, are described in this chapter in order to introduce the basic concepts of radiation applicable to musical instruments. In each case, the radiation field is characterized in terms of sound pressure, directivity, acoustic intensity, and sound power. The dependence of the pressure amplitude with respect to distance and frequency is highlighted. Pulsating and oscillating spheres are used as reference examples to illustrate these concepts. Another interest of the elementary sources follows from the fundamental Kirchhoff–Helmholtz theorem, which states that any extended source can be represented as a distribution of elementary sources. This result forms the basis of the calculation of the acoustic field radiated by a musical instrument with arbitrary geometry. Particular attention is also paid to the radiation of sound tubes, either isolated or with mutual influence due to their proximity.

12.1 Introduction: Acoustical Radiation of Musical Instruments

Musical instruments are primarily designed for radiating sound power: this is a necessary condition for allowing the audience to listen to music! A good knowledge on the radiation mechanisms is also essential for the sound engineer, who is in charge of recording a concert with only a finite number of microphones. The sound that reaches the listener (or the microphones) not only depends on the properties of the sources (the musical instruments), but also on the properties of the listening space, and on the position of the listener (resp. the microphones) in the room.

A. Chaigne (✉)
Institute of Music Acoustics, University of Music and Performing Arts Vienna (MDW), Anton-von-Webern-Platz 1, 1030 Vienna, Austria
e-mail: antchaigne@gmail.com

J. Kergomard
CNRS Laboratoire de Mécanique et d'Acoustique (LMA), 4 impasse Nikola Tesla CS 40006, 13453 Marseille Cedex 13, France
e-mail: kergomard@lma.cnrs-mrs.fr

A. Chaigne, J. Kergomard, *Acoustics of Musical Instruments*, Modern Acoustics and Signal Processing, DOI 10.1007/978-1-4939-3679-3_12

In this fourth part of the book, we limit ourselves to the physical description of the radiation of the instruments, leaving aside the questions linked to the acoustics of the room and on the psychoacoustical aspects of the sound perceived by the listeners. However, before starting this study, a rapid overview is made on the parameters to be considered, alternatively from the point of view of the player, the listener, and the sound engineer.

An instrument has to be heard. From the point of view of the physicist, this implies that it can produce sufficient sound power. In an orchestra, or in a chamber music ensemble, another linked question is the level balance between all sections of instruments. This, in turn, determines, for example, the total number of violin players compared to the number of trumpet or clarinet players in an orchestra. We will not go further into these considerations which, as one can imagine, also largely depend on aesthetic choices and on the work performed.

The spatial distribution of the radiated sound and the directivity of the instrument also are important aspects of radiation. During a concert, some instruments, such as the trumpet or the trombone, for example, radiate in restricted emitting cones. In what follows, we will see that the directivity of a given instrument strongly depends on frequency, and thus varies substantially from bass to treble range.

For the player, one important feature of the instrument is the ratio between the input mechanical power and the acoustical power at the "output." This determines the playability of the instrument: in a number of situations, some notes are more difficult to play than others. As a consequence, the sound level can be very heterogeneous over the complete frequency range of the instrument. In terms of physics, attempt will be made to model the relationships between the input mechanical quantities (blow velocity, plucking force, bow pressure, key velocity,...) and the sound pressure.

These are also central questions for the instrument maker. The physical approach of the instrument must serve as a guide for the selection of construction parameters (geometry, materials,...). The function of the developed models is to establish clear links between these parameters and the sound qualities of the instrument: sound level, dynamic range, directivity, homogeneity, and playability.

To finish with this preamble, let us add a few words on contemporary music, with focus on those which make a large use of virtual instruments and synthesizers. In this case, the sound does not result from structural-acoustics coupling between instrument's body and air, but is rather obtained by transduction through loudspeakers. The question of sound level is less critical here, since it is always possible to amplify the electric signal, within the limits imposed by the linear range of the transducers. However, the problem of directivity is still present as well as the question of distribution of these virtual sources in a symphonic orchestra.

12.1.1 General Problem of Radiation

12.1.1.1 Musical Sound Sources

The radiation mechanisms are specific for each musical instrument. However, three basic mechanisms (or source types) are present, to a lesser or greater extent, in each family of instruments [10]:

1. For the sources of **type 1**, the sound results from the variation with time of a *volume flow*. The academic example is the *pulsating sphere* that can be illustrated by the oscillations of a air bubble in water. In musical acoustics, the lowest mode of a kettledrum struck by a mallet in its center, or the radiation at the end of a tube (below the cut-off frequency), are examples of such sources (see Fig. 12.1). In this case the continuity equation (1.109), presented in Part I of this book, is written:

$$\frac{1}{c^2}\frac{\partial p}{\partial t} + \rho \,\mathrm{div}\, \boldsymbol{v} = m, \tag{12.1}$$

   where $m = \rho q$ represents the *mass flow*, or, equivalently, the volume and time density of mass injected in the surrounding fluid.
2. In **type 2** sources, the sound results from local variations of forces exerted on the particles of the fluid, with a zero volume velocity. The standard models of such sources are the *oscillating disk* or the *oscillating sphere*. In musical acoustics, the lowest flexural mode of a xylophone beam, the 11 mode of a kettledrum or of a guitar plate are examples of type 2 sources (see the Fig. 12.1). In general, external force densities are present not only on oscillating sources, but also when sound waves are reflected on a rigid surface. One example was given in Chap. 10 for the flutes. In the presence of external force density $\boldsymbol{f}$, the linearized Euler equation in the fluid becomes

$$\rho \frac{\partial \boldsymbol{v}}{\partial t} + \mathbf{grad}\, p = \boldsymbol{f}\,. \tag{12.2}$$

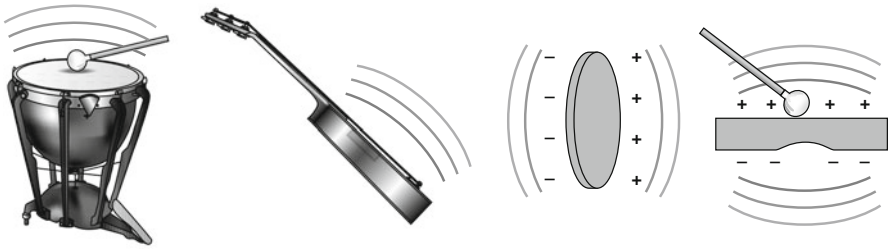

Fig. 12.1 (*Left*) Examples of sources of type 1: lowest modes of a kettledrum and of a guitar plate. (*Right*) Examples of sources of type 2: oscillating disk, first flexural mode of a xylophone beam, without its resonator

where $\boldsymbol{f} = \rho \boldsymbol{F}$ ($\boldsymbol{F}$ is a mass density of force). Eliminating the acoustic velocity $\boldsymbol{v}$ between these two equations yields the heterogeneous wave equation (i.e., with a source term):

$$\frac{1}{c^2}\frac{\partial^2 p}{\partial t^2} - \Delta p = \frac{\partial m}{\partial t} - \operatorname{div} \boldsymbol{f} \,. \tag{12.3}$$

In Eq. (12.3), the two types of sources are present in the right-hand side. It can be seen that the mass term produces sound only if it varies with time. Conversely, the force term produces some sound under the condition of spatial variation.

3. Finally, sources of **type 3** exist in a viscous fluid, and are due to the presence of shear stresses. The formulation of these source terms is obtained by taking the viscosity forces and the convective acceleration (nonlinear terms) in the equations. These terms govern, for example, the origin of jet noise in aeroacoustics [see Eq. (10.30) and Sect. 10.4 in Chap. 10] [26].

12.2 Elementary Sources

Elementary sources are limiting cases that are often very useful, to a first approximation, in order to describe complex sources such as musical instruments.

The pulsating sphere is a good archetype of a perfectly omnidirectional source, which means that the amplitude of the sound pressure only depends on the distance from the source, and not on the angle of observation. The example of the air bubble in water was given in the previous paragraph, but it is not very "musical"! In musical acoustics, the radiation of the guitar soundhole, or of the end of a tube, also can be considered as omnidirectional, at least in a given frequency range. If the radiation field is omnidirectional in an half-space (or in the fraction of the acoustic space), then models of pulsating half-sphere or fractional pulsating spheres can be applied. In what follows, this simple model will be used to introduce the basic concepts of acoustic intensity, radiating power and impedance, and to define the concepts of both near and far fields.

A *monopole*, or point source, can be viewed as the theoretical limit of a pulsating sphere, when its radius tends to zero. It is an idealized system which is not feasible in practice. However, one can build reasonable approximate monopole sources under the condition that their dimensions are kept small compared to the wavelength and/or the distance to the observer (listener).

In contrast with the pulsating sphere (source of type 1), the volume of an oscillating sphere (or of an oscillating disk) does not change during its motion and it will be seen below in this chapter that it corresponds to a type 2 source. The limiting case of such sources yields another elementary source called *dipole*. A dipole is a directional source. It will be shown that a dipole with the same amplitude as the one of a monopole radiates the low frequencies less efficiently. In musical acoustics a xylophone beam, or an oscillating string, can be conveniently described by linear arrays of dipoles [15].

One major interest of such point sources lies in the fact that extended sources can be viewed as distribution of elementary sources. This is one essential result of the Kirchhoff–Helmholtz theorem that will be demonstrated at the end of the present chapter. This theorem also forms the theoretical basis of numerical techniques such that the *Boundary Element Method* which are of current use for the computation of acoustic radiation.

In this chapter, the main properties of the elementary acoustic sources are reviewed, without the details of the mathematical derivations. The reader is invited to consult the numerous textbooks available on these topics (see, for example, [31]). Emphasis is put instead on the consequences of these properties in the particular cases of musical instruments. Most derivations are made in the frequency domain, although some examples are intentionally treated in the time domain.

12.3 Pulsating Sphere

The most simple example of a "type 1" source is the pulsating sphere. Due to the spherical symmetry of the problem, the radiation phenomena can be described analytically with only one spatial coordinate. A sphere with radius a and given radial velocity $V_a(\omega)$ along its periphery (S) is described here in the frequency domain (Fig. 12.2). The amplitude of the radial motion is supposed to be small compared to the radius.

12.3.1 Pressure and Velocity Fields

Using the wave equation expressed in spherical coordinates, as seen in Sect. 7.4.1 in Chap. 7, we get the expression of the radiated pressure field at a distance r from the center of the sphere. In what follows, the pressure field inside the sphere is ignored (it might lead to nonlinear effects in the vicinity of the center whose is beyond the

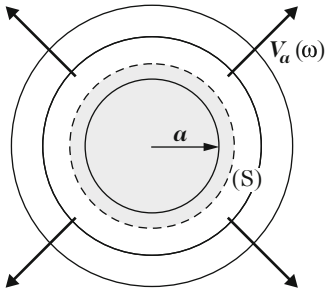

Fig. 12.2 A pulsating sphere of radius a is vibrating radially with angular frequency ω and velocity $V_a(\omega)$ along its periphery (S): the resulting pressure at a given distance from the center of the sphere is identical in all directions

scope of this book) and we concentrate on the outside pressure in free space. From the general solution, the pressure at a distance r can be expressed as a function of the surface pressure $P(a)$ as follows[1]:

$$P(r) = P(a)\frac{a}{r}e^{-jk(r-a)}. \tag{12.4}$$

Using the specific admittance in a [Eq. (7.79)], we get the pressure $P(r)$ as a function of the acoustic velocity which is, by continuity, equal to V_a. Introducing the volume velocity of the sphere $U = 4\pi a^2 V_a$, we get

$$P(r) = \frac{\rho c}{4\pi a^2}\frac{a}{r}U\frac{jka}{1+jka}e^{-jk(r-a)}\ . \tag{12.5}$$

The first term in this expression is the *characteristic acoustical impedance* of the source $Z_c = \frac{\rho c}{4\pi a^2}$. The second term a/r characterizes the *spherical expansion in free field* (or $1/r$ law). The term $\frac{jka}{1+jka}$ governs the frequency dependence of the pressure. If the characteristic dimension of the sphere (the radius a, here) is small compared to the acoustical wavelength ($ka \ll 1$), then the magnitude of the sound pressure is of the same order as ka. Conversely, for the "small" wavelengths ($ka \gg 1$), in the "high" frequency range, the magnitude of P becomes independent of frequency. Finally, the exponential term expresses the delay of propagation between the vibrating surface of the sphere and the observation point. This delay takes the form of a phase shift in the frequency domain. Figure 12.3 shows the variations of the squared pressure modulus as a function of frequency for a given source at a given fixed point in space.

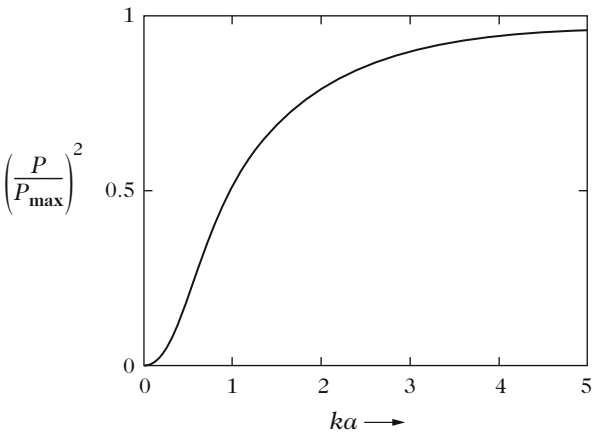

Fig. 12.3 Squared modulus of the pressure radiated by a pulsating sphere as a function of the dimensionless frequency ka

[1] In all the following expressions, the time dependence of the acoustical quantities are omitted, for simplicity. Thus, $P(r, \omega)$ is denoted $P(r)$.

Using again the expression of the admittance in r [Eq. (7.79)] now yields

$$V(r) = \frac{U}{4\pi a^2}\frac{a^2}{r^2}\frac{1+jkr}{1+jka}e^{-jk(r-a)}\,. \tag{12.6}$$

It can be checked in (12.6) that the continuity condition of the radial velocity is fulfilled in $r = a$. When the observation point is located far from the source ($kr \gg 1$, in terms of wavelength), then the modulus of the acoustic velocity decreases proportionally to $1/r$ as the sound pressure. In this case $P(r) \simeq \rho c V(r)$, which means that the radiated wave at a large distance from the source behaves like a plane wave. In contrary, if $kr \ll 1$ (in the near field of the source), the acoustic velocity decreases as $1/r^2$.

These results illustrate different important cases of approximations which are frequently encountered when studying the radiation of sound sources:

- *Approximation at the emission* depending on the ratio between the dimensions of the source and the acoustic wavelength (discussion on the parameter ka in the case of the pulsating sphere)
- *Approximation at the reception* depending on the ratio between the source-receiver distance and the wavelength (discussion on the parameter kr in the case of the pulsating sphere)

In some case, we might also consider *purely geometrical* approximations, for a given wavelength, where a comparison has to be made between the source-receiver distance and the characteristic dimension of the source. For the pulsating sphere, for example, this refers to approximations involving the ratio a/r.

12.3.2 Acoustic Intensity and Sound Power

From the expressions of pressure and acoustic velocity in the frequency domain, the mean value of the acoustic intensity is derived.[2] In the case of the pulsating sphere, the acoustic intensity is radial (as the velocity) and its modulus is equal to:

$$I(r) = \frac{1}{2}\Re e\{P(r)V^*(r)\} = \frac{|U|^2}{4\pi r^2}\frac{\rho c}{2S}\frac{k^2a^2}{1+k^2a^2}, \tag{12.7}$$

where $S = 4\pi a^2$ is the emitting surface.

One can see that the mean acoustic intensity decreases in $1/r^2$, which is in accordance with the property of spherical expansion. The mean acoustic power corresponds to the flow of the acoustic intensity vector through a closed surface surrounding the source. Taking advantage of the spherical symmetry, the power is computed on a spherical surface Σ with radius r, which yields

[2] In this chapter, capital letters are used for all quantities expressed in the frequency (Fourier) domain. Recall that the concept of mean power only has a signification in the frequency domain.

$$\mathscr{P}_r = \int_\Sigma I(r) d\Sigma = 4\pi r^2 I(r) = \frac{\rho c\,|U|^2}{2S} \frac{k^2a^2}{1+k^2a^2}\,. \tag{12.8}$$

The quantity $\mathscr{P}_r$ is independent of r, which is in accordance with the principle of energy conservation, since no dissipation has been introduced in the model, neither on the source, nor during the propagation. The evolution of the acoustic power with the reduced number ka is identical to the squared modulus of the pressure (see the Fig. 12.3). For a given volume velocity U, the sound power radiated by the spherical sphere is proportional to the square of frequency as long as $ka \ll 1$, and tends to the asymptotic limit $\mathscr{P}_{\max} = \frac{\rho c|U|^2}{2S}$ for $ka \gg 1$.

12.3.3 Force Exerted by the Fluid on the Sphere: Radiation Impedance

Let us now examine the different acoustic quantities in the vicinity of the pulsating sphere. The *radiation impedance* is defined as the ratio between the surface pressure and the volume velocity in $r = a$. We have

$$Z_r = \frac{P(a)}{SV(a)} = \frac{\rho c}{S}\frac{jka}{1+jka} = \frac{\rho c}{S}\left[\frac{k^2a^2}{1+k^2a^2} + j\frac{ka}{1+k^2a^2}\right] = R_r + jX_r\,. \tag{12.9}$$

Comparing (12.9) and (12.8), one can see that the acoustic power can be written equivalently:

$$\mathscr{P}_r = \frac{|U|^2}{2} R_r\,. \tag{12.10}$$

In other words, the acoustic power radiated by the sphere is proportional to the real part of the radiation impedance (or *radiation resistance*) R_r. The imaginary part of the radiation impedance (or *reactance*) X_r is written:

$$X_r = \frac{\rho c}{S}\frac{ka}{1+k^2a^2}\,. \tag{12.11}$$

One can see that X_r has the form of an acoustic mass. This mass depends on frequency, except for $ka \ll 1$. In this latter case, the mass is constant and is equal to $\frac{\rho a}{S}$. The reactance corresponds to the inertial forces that are to be overcome by the sphere during its motion, and to the fluctuating power exchanged between the source and the near field (see Chap. 1). In summary, the radiation impedance yields useful information on the radiated sound power and on the reaction of the fluid on the acoustic source. If the sphere radiates in a finite space (room, cavity), then the reactance might also contain an elastic term which represents the influence of the compressibility of the enclosed fluid.

12.3.4 Concept of Point Source

12.3.4.1 First Approach

Imagine now that the radius of the pulsating sphere vanishes, while keeping a constant volume velocity U. As a result, we obtain a omnidirectional point source, centered at point $r = 0$, called *monopole*. The pressure (12.5) becomes

$$P(r) = j\omega\rho U G(r) \quad \text{with} \quad G(r) = \frac{e^{-jkr}}{4\pi r} . \tag{12.12}$$

The function $G(r)$ is the *Green's function* in free space. More generally, if $\boldsymbol{r}'$ denotes the position of the point source and $\boldsymbol{r}$ the one of the observer ($\boldsymbol{r}$ and $\boldsymbol{r}'$ are vectors), one writes

$$G(\boldsymbol{r}|\boldsymbol{r}') = G(\boldsymbol{r}'|\boldsymbol{r}) = \frac{e^{-jk|\boldsymbol{r}-\boldsymbol{r}'|}}{4\pi\,|\boldsymbol{r}-\boldsymbol{r}'|} . \tag{12.13}$$

This expression shows the important *reciprocity* property of the Green's function which means that the expression of the pressure is unchanged through permutation of the respective coordinates of both the source and receiver.

In the time-domain, the operator $j\omega$ corresponds to a time derivative, while the operator $\exp(-jkr)$ corresponds to a delay r/c. As a consequence, the pressure $p(r,t)$ generated by the monopole is written:

$$p(r,t) = \frac{\rho}{4\pi r}\frac{d}{dt}u\left(t - \frac{r}{c}\right) . \tag{12.14}$$

In Eq. (12.14), one can see that an acoustic pressure exists only if the *time derivative of the volume velocity* is different from zero. A sphere moving at constant speed, for example, does not create sound.[3] It is also observed that the pressure still decreases in $1/r$. It is finally not surprising to see that the pressure (which is nothing but a surface force density) is proportional to an acceleration, following Newton's second law.

12.3.4.2 Second Approach

The mathematical tool that describes the point source is the Dirac delta distribution δ. Imagine now that a point source with volume velocity $u(t)$ is placed at the origin of the axes (in $r = 0$). In order to establish a link with the wave

[3]This remark might be surprising and seems to contradict everyday experience where a vehicle rolling at constant speed creates aerodynamical noise. In fact, this noise is due to the viscous forces in the fluid, which are not taken into account in the present model.

equation (12.3), one can write that the mass flow is defined as:

$$m = \rho\, u(t)\, \delta(r)\ . \tag{12.15}$$

The Helmholtz equation is then written:

$$\Delta P + k^2 P = -j\omega\rho U(\omega)\delta(r)\ . \tag{12.16}$$

In order to solve (12.16), this equation is integrated on a sphere of radius ε with $\varepsilon \to 0$ (see Fig. 12.4). Due to the spherical symmetry, one can write $P(r) = \frac{A}{r}\exp(-jkr)$, for $r \neq 0$. Denoting $\mathcal{V}$ the volume of the sphere around the source, the integration of (12.16) is written:

$$A\int_{\mathcal{V}} \Delta\left(\frac{e^{-jkr}}{r}\right) d\mathcal{V} + A\int_{\mathcal{V}} k^2 \frac{e^{-jkr}}{r} d\mathcal{V} = -j\omega\rho U\ . \tag{12.17}$$

After some manipulations, this equation can be transformed as follows:

$$A\int_S \mathbf{grad}\left(\frac{e^{-jkr}}{r}\right).\boldsymbol{n}\, dS + A\int_0^{\varepsilon} k^2 4\pi r e^{-jkr} dr = -j\omega\rho U, \tag{12.18}$$

where (S) is the surface of the sphere of radius ε and $\boldsymbol{n}$ the normal vector oriented towards the external field (see Fig. 12.4). As ε tends to zero, the first integral in (12.18) tends to -4π, and the second integral vanishes. One obtains

$$A = \frac{j\omega\rho}{4\pi} U \quad \text{and} \quad P(r) = j\omega\rho U G(r)\ . \tag{12.19}$$

One find then again the intuitive solution previously obtained for a finite pulsating sphere as the radius tends to zero. By the way, one shows that if P is a solution of (12.16), then the Green's function $G(\boldsymbol{r}|\boldsymbol{r'})$ is a solution of the equation:

$$\Delta G(\boldsymbol{r}|\boldsymbol{r'}) + k^2 G(\boldsymbol{r}|\boldsymbol{r'}) = -\delta(\boldsymbol{r} - \boldsymbol{r'})\ . \tag{12.20}$$

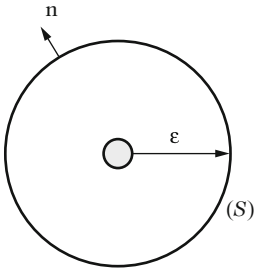

Fig. 12.4 Integration of the Helmholtz equation with a point source

In what follows, the set of both Eqs. (12.16) and (12.20) will be used for calculating the pressure field radiated by any source.

12.3.4.3 Acoustic Power Radiated by a Monopole

In order to calculate the sound power radiated by a monopole, the acoustic intensity is integrated over a spherical surface around the source, as it has been done for the pulsating sphere. Alternatively, one can also use the expression (12.8) and calculate its limit when $ka \ll 1$. In both cases, one gets

$$\mathscr{P}_r = \frac{\rho c k^2 |U|^2}{8\pi} = \frac{\rho \omega^2 |U|^2}{8\pi c} . \tag{12.21}$$

which indicates, among other things, that the power radiated by a monopole is proportional to the square of frequency.

12.3.5 Monopole Arrays

In order to extend the results of the previous paragraph, let us now consider a discrete set of monopoles distributed in space (see Fig. 12.5). This array can be seen as a cloud of active points. Applying the principle of superposition which is valid in linear acoustics, one can derive the resulting field at a given point M of coordinates $\boldsymbol{r}$ just by summing the contributions of the n sources of volume velocities U_n:

$$P(\boldsymbol{r}) = \frac{j\omega\rho}{4\pi} \sum_n U_n \frac{e^{-jkR_n}}{R_n} = \frac{j\omega\rho}{4\pi} \sum_n U_n \frac{e^{-jk|\boldsymbol{r}-\boldsymbol{r_n}|}}{|\boldsymbol{r}-\boldsymbol{r_n}|} . \tag{12.22}$$

This result can be generalized to the case of a continuous distribution of monopoles with elementary volume velocities UdS distributed over a surface $\mathscr{S}$:

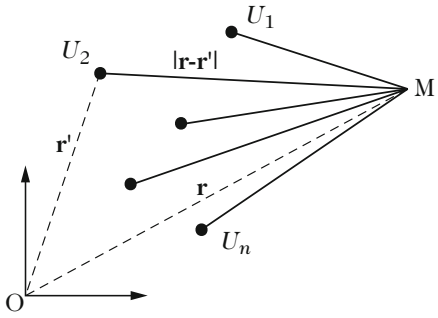

Fig. 12.5 Discrete arrays of monopoles

$$P(\boldsymbol{r}) = \frac{j\omega\rho}{4\pi}\int_{\mathscr{S}} U(\boldsymbol{r}')\,\frac{e^{-jk|\boldsymbol{r}-\boldsymbol{r}'|}}{|\boldsymbol{r}-\boldsymbol{r}'|}d\mathscr{S}, \tag{12.23}$$

whose equivalent time-domain formulation is given by:

$$p(\boldsymbol{r},t) = \frac{\rho}{4\pi}\frac{d}{dt}\int_{\mathscr{S}} \frac{1}{|\boldsymbol{r}-\boldsymbol{r}'|}\,u\left(\boldsymbol{r}', t-\frac{|\boldsymbol{r}-\boldsymbol{r}'|}{c}\right)\,d\mathscr{S}\,. \tag{12.24}$$

Important Remark Equation (12.24) is not valid if $\mathscr{S}$ corresponds to the surface of a finite structure with a finite volume. In this latter case, the waves radiated by the structure are reflected by its own surface, and this phenomenon has to be taken into account.

12.3.5.1 Large Distance Approximations

let us denote L a characteristic dimension of the monopolar distribution. For $r \gg L$, the pressure at a distance r from the source in (12.24) can be simplified, considering that $|\boldsymbol{r}-\boldsymbol{r}'| \simeq r$. A first level of approximation (we will denote it *modulus* approximation) is obtained by simplifying the denominator only:

$$p(\boldsymbol{r},t) = \frac{\rho}{4\pi r}\frac{d}{dt}\int_{\mathscr{S}} u\left(\boldsymbol{r}', t-\frac{|\boldsymbol{r}-\boldsymbol{r}'|}{c}\right)d\mathscr{S}\,. \tag{12.25}$$

For rapidly varying signals (with significant energy in the "high" frequency range) the phase terms can be significant and cannot be neglected, even in the case of small propagation delays between the sources. These delays may alter the waveform at the receiver substantially. Conversely, for slowly varying signals with a significant energy level in the "low" frequency range, an higher level of approximation (let us denote it *phase* approximation) leads to the expression:

$$p(\boldsymbol{r},t) = \frac{\rho}{4\pi r}\frac{d}{dt}\int_{\mathscr{S}} u\left(\boldsymbol{r}', t-\frac{\boldsymbol{r}}{c}\right)d\mathscr{S}\,. \tag{12.26}$$

In this case, the pressure is equivalent to the one radiated by a unique monopole whose total volume velocity is the sum of all elementary volume velocities. However, one should keep in mind that this equivalence is only valid in restrictive situations which depend on the assumptions made on the geometry of the source distribution and on the properties (spectral content) of the emitted signal.

12.3.5.2 Acoustic Power Radiated by a Set of Coherent Monopoles

For a set of sources radiating coherent acoustic signals simultaneously, the acoustic power radiated by each source is affected by the presence of the other sources (see, for example, [14]).

One can think, for example, of the simultaneous emission of pressure by the two main sources of a flute (mouth and open end) for a given note, as seen in Chap. 7. This phenomenon is now illustrated in a simple case involving two monopoles S_1 and S_2 separated by a distance d, and with given volume velocities U_1 and U_2. The results can be generalized to the case of multiple sources.[4]

The far field pressure (at point M) can be calculated using an approximation of the type (12.26). We denote θ the angle between the vector $\boldsymbol{OM} = \boldsymbol{r}$ and the source axis (see the Fig. 12.6). With a first-order expansion (in terms of the ratio d/r), the distance between the source S_1 and the observation point M is $|r - r_1| \simeq r + \frac{1}{2} d \cos\theta$, whereas it is equal to $|r - r_2| \simeq r - \frac{1}{2} d \cos\theta$ for the distance between S_2 and M.

$$P(r) = \frac{j\omega\rho}{4\pi r} e^{-jkr} U(\theta) \text{ where } U(\theta) = U_1 e^{-j\frac{kd}{2}\cos\theta} + U_2 e^{+j\frac{kd}{2}\cos\theta} . \qquad (12.27)$$

Fig. 12.6 Two monopoles.
For a dipole: $U_2 = U = -U_1$

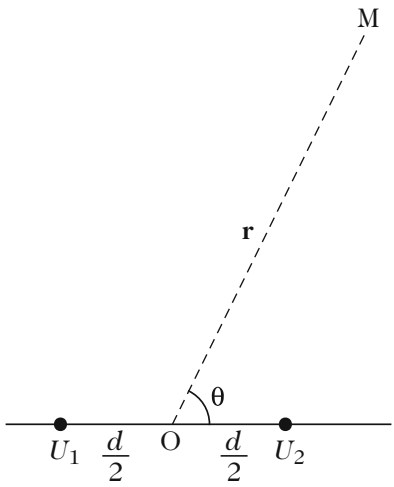

[4]For the sake of simplicity, the following derivations are made in the case of given volume velocities. However, one has to be aware of the fact that, in numerous cases, the two sources are not independent and are linked together by means of a transfer function. This is, for example, the case for the side holes of wind instruments interacting through the resonator, or for the volume velocities of plate and sound hole in stringed instruments that are coupled by the air cavity (see Chap. 6).

The far field behavior of these two sources is thus equivalent to the one of a single monopole, though with a directivity $U(\theta)$ depending on the reduced wavenumber kd. In order to calculate the total acoustic power radiated by both sources, one has to calculate[5] the acoustic intensity on a sphere with radius r. Using the notations $U_{1,2} = |U_{1,2}| \exp(j\varphi_{1,2})$ and $\varphi = \varphi_2 - \varphi_1$, we have

$$\mathscr{P}_r = \frac{\rho c k^2}{8\pi} \left[|U_1|^2 + |U_2|^2 + 2|U_1||U_2| \frac{\sin kd}{kd} \cos\varphi \right] . \tag{12.28}$$

The power is always positive, because the free field can be seen as an absorbing medium at the infinity, and thus the outgoing pressure never comes back to the source. The term in $|U_1||U_2|$ is the *interaction* term. Let us first consider two sources of identical amplitudes in the low-frequency range ($kd \ll 1$). if the sources are in phase, the interferences are constructive, and the sound power is equal to four times the power radiated by a single source ($+ 6\,\mathrm{dB}$). If these sources are in antiphase ($\varphi = \pi$), the sound power is close to zero. By expanding $\sin kd$ to the third order in kd, we then find the expression of the sound power radiated by a dipole (see the next section). One well-known illustration is the case of two loudspeaker systems in antiphase.

Let us now examine how the power is distributed among both sources [14]: depending on the values taken by φ, the sound power due to the presence of the second monopole can either increase or decrease. Moreover, is the amplitude ratio $|U_2/U_1|$ is larger than unity, the power can even become negative, which means that the second monopole is absorbing part of the acoustic energy: it behaves then like a *sink* and not like a source.

Directivity of a Linear Array of Monopoles

One main consequence of linear arrays of monopoles is that the directivity increases compared to the case of a single monopole. One can take benefit of this property in electroacoustics: an antenna of microphones is used, for example, if the purpose is to record a source in a restrictive solid angle. Such a process is very useful in order to record situated at a large distance from the microphones, since it reduces the influence of sideways ambient noise considerably. Reciprocally, loudspeakers arrays are used with the purpose of radiating sound in a restrictive region of space. The directivity of arrays is a joint property of both sources and receivers.

[5] On should integrate over the surface $r =$constant :

$$I(r,\theta) = \frac{1}{2} \frac{k^2 \rho c}{(4\pi r)^2} |U(\theta)|^2 \quad \text{where} \quad |U(\theta)|^2 = |U_1|^2 + |U_2|^2 + 2|U_1||U_2| \cos\left[kd\cos\theta + \varphi\right]$$

which amounts to calculate the integral $2\pi r^2 \int_0^\pi |U(\theta)|^2 \sin\theta d\theta$. This calculation is straightforward since $\sin\theta$ is the derivative of the θ-function appearing in $\cos\left[kd\cos\theta + \varphi\right]$.

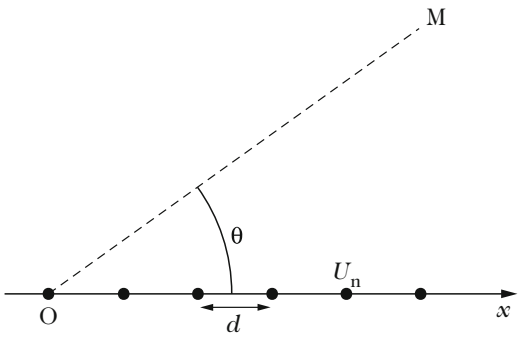

Fig. 12.7 Linear array of monopoles

Musical instruments do not escape this rule: a slender structure (like a xylophone bar) vibrating on a high flexural mode can be viewed as a linear array of sources.

Another illustrative example is the association of several regularly distributed open holes in wind instruments. In order to determine theoretically the directivity resulting from the association of point sources, we calculate it below for an array composed by N monopoles with velocities U_n, equally distributed on the x axis, with a distance d between consecutive sources (see Fig. 12.7). It is assumed here that all sources have the same amplitude, but that there is a constant phase shift between consecutive sources:

$$U_n = U \exp\left[-j(n-1)\varphi\right].$$

Using a first-order expansion of $|\boldsymbol{r} - \boldsymbol{r}_n|$ in (12.22), and defining θ as the angle between the x-axis and the vector $\boldsymbol{r} = \boldsymbol{OM}$, where M is the observation point, the pressure is written:

$$P(r,\theta) = \frac{j\omega\rho_0 U e^{-jkr}}{4\pi r} \sum_{n=1}^{N} e^{j(n-1)(kd\cos\theta-\varphi)} . \tag{12.29}$$

Denoting then $\Theta = (kd\cos\theta - \varphi)$, the directivity of the array is given by:

$$\mathscr{D}(\theta) = \frac{1}{N}\frac{e^{-2jN\Theta}-1}{e^{-2j\Theta}-1} = \frac{\sin N\Theta}{N\sin\Theta} . \tag{12.30}$$

Examining (12.30) shows that the main lobe of the directivity pattern becomes narrower as N increases (see Fig. 12.8).

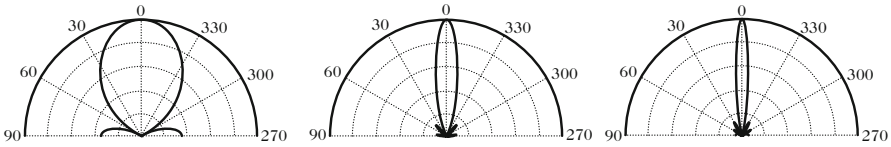

Fig. 12.8 Directivity $D(\theta)$ of the array [see Eq. (12.30)] for different numbers N of monopoles: (*left*) $N = 3$; (*center*) $N = 10$; (*right*) $N = 20$

12.4 Oscillating Sphere

We now turn to the sources with a global zero volume velocity, but which are subjected to a force density $\boldsymbol{f}$ by the surrounding fluid during their motion. In this case, the heterogeneous wave equation (12.3) shows that the divergence of the force density must be different from zero in order to generate sound. An oscillating source meets these requirements, since its motion creates an overpressure in front and a decrease of pressure at the back. In total, this produces a spatial heterogeneity of the force field in the vicinity of the source that creates a nonzero divergence term. At the same time, the total sum of the volume velocities is zero. In order to compare the properties of the oscillating sphere with those of the pulsating sphere, the main results are briefly reviewed below. As done previously, bringing the radius of the sphere close to zero allows to define a dipole, or elementary oscillating source.

12.4.1 Pressure and Velocity Field

Given $v_0(t)$ the oscillating velocity of a sphere of radius a (see Fig. 12.9), and $V_0(\omega)$ its Fourier transform. θ is the angle between the direction of the oscillation and the radial velocity at a given point of the sphere surface. The equation of continuity at the interface between fluid and solid allows to write:

$$V_r(a) = V_0 \cos\theta. \tag{12.31}$$

As for the pulsating sphere, the acoustic pressure and velocity fields are obtained by combining the wave equation with the Euler equation. We find

$$P(r,\theta) = \rho c V_0 \cos\theta \frac{a^2}{r^2}\left[\frac{jka(1+jkr)}{2+2jka-k^2a^2}\right] e^{-jk(r-a)}\,. \tag{12.32}$$

The main difference with the pulsating sphere is the presence here of the *directivity factor* $\cos\theta$ in the expression of the pressure (see Fig. 12.10). As a consequence, the pressure is maximum in the direction of the oscillation, and zero

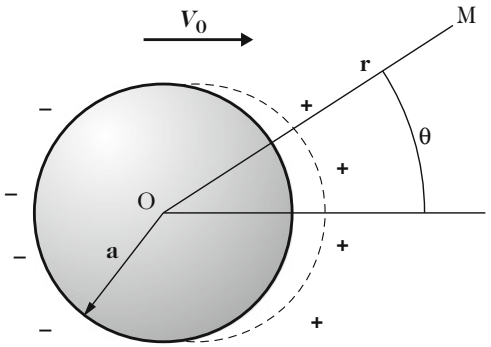

Fig. 12.9 A rigid oscillating sphere creates an overpressure in front and a decrease of pressure at the back, during its motion. In the median plane, overpressure and decrease of pressure are equal and opposite in signs, and thus the resulting pressure is equal to zero

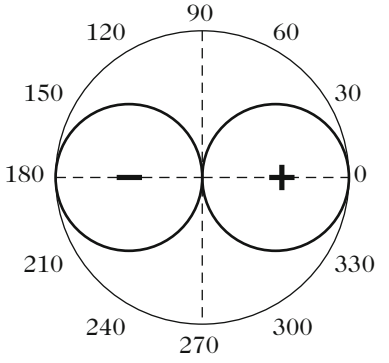

Fig. 12.10 Pressure directivity of an oscillating sphere

in the plane perpendicular to it. A small distances ($kr \ll 1$), the pressure varies as $1/r^2$, and as $1/r$ for $kr \gg 1$. Finally, we have the propagation term $\exp[-jk(r-a)]$.

The acoustic velocity vector has now two components, in the directions $\boldsymbol{e_r}$ and $\boldsymbol{e_\theta}$, respectively (see Fig. 12.11):

$$\begin{cases} V_r(r,\theta) = V_0 \cos\theta \dfrac{a^3}{r^3} \dfrac{2+2jkr-k^2r^2}{2+2jka-k^2a^2} e^{-jk(r-a)}, \\ V_\theta(r,\theta) = V_0 \sin\theta \dfrac{a^3}{r^3} \dfrac{1+jkr}{2+2jka-k^2a^2} e^{-jk(r-a)}. \end{cases} \tag{12.33}$$

In the near field ($kr \ll 1$), both components of the velocity vary as $1/r^3$. In the far field ($kr \gg 1$), the radial component varies as $1/r$. The specific impedance is equal to ρc, and the component along $\boldsymbol{e_\theta}$ varies as $1/r^2$.

12.4.2 Acoustic Intensity and Radiated Pressure

The $\boldsymbol{e_\theta}$-component of the intensity is zero. Its radial component is given by:

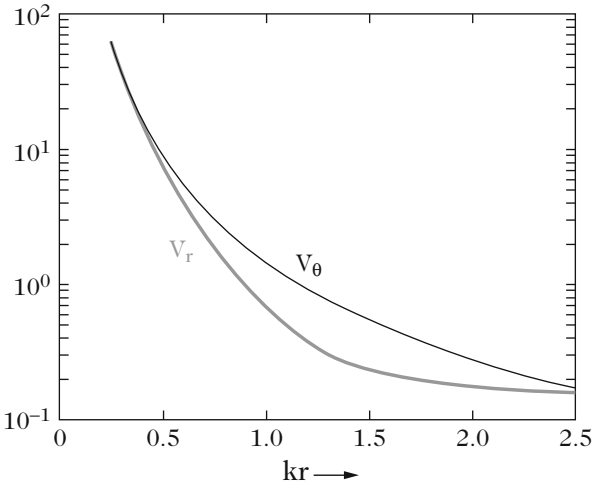

Fig. 12.11 Acoustic velocity radiated by an oscillating sphere

$$I_r(r,\theta) = \frac{1}{2} Re\,\{PV_r^*\} = \frac{1}{2}\rho c\,\frac{a^2}{r^2}\,\frac{k^4a^4}{1+k^4a^4}\,|V_0|^2\cos^2\theta\ . \tag{12.34}$$

The radiated power is derived:

$$\mathscr{P}_r = \int_S I_r(r,\theta)\,dS = \rho c\,\frac{2\pi a^2\,|V_0|^2}{3}\,\frac{k^4a^4}{1+k^4a^4}\ . \tag{12.35}$$

If the acoustic wavelength is larger than the dimensions of the source ($ka \ll 1$), then the radiated power is proportional to ω^4. This means that, for given radius and velocity magnitude, an oscillating sphere is less efficient for radiating sound in the low-frequency domain, compared to a pulsating sphere. Using Eqs. (12.8) and (12.35), it is found that the ratio η between both acoustic powers, for a given oscillation velocity V_0, is given by:

$$\eta = \frac{(\mathscr{P}_r)_{SO}}{(\mathscr{P}_r)_{SP}} = \frac{k^2a^2}{3}\,\frac{1+k^2a^2}{1+k^4a^4}\ , \tag{12.36}$$

which yields $\eta \simeq k^2a^2/3$ for the sources of small dimensions $ka \ll 1$.

This reduction of radiated power at low frequencies is the consequence of destructive interferences between the acoustic waves generated in the front and at the back, respectively. If the wave at the back is "eliminated" in an absorbing box, as made in most loudspeaker systems, the radiating properties of the system become closer to a those of a monopole and is thus more efficient at low frequencies. It is exactly what happens also in drums (timpani, bass drums,...).

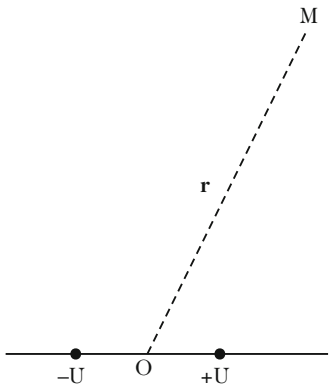

Fig. 12.12 Elementary dipole

12.4.3 Concept of Elementary Dipole

12.4.3.1 First Approach

Bringing the radius of the sphere in (12.32) close to zero yields the expression of the sound pressure generated by an oscillating point source (or dipole) (Fig. 12.12):

$$P(r,\theta) = j2\pi a^3 \omega \rho V_0 \left(jk + \frac{1}{r}\right) G(r) \cos\theta \ . \tag{12.37}$$

The reader can check that this expression is identical to the one obtained by calculating the pressure radiated by a set of two monopoles of equal volume velocity and opposite signs $+U/-U$, where $d = 2a$ is the distance between them (see Fig. 12.6) and where

$$U = \int_S \boldsymbol{V_0}.\boldsymbol{n}\, dS = \pi a^2 V_0 \ . \tag{12.38}$$

Defining now $D_d = j2a\omega\rho U = jk\rho cUd$ as the *moment* of the dipole[6] and using the definition of the Green's function in free space $G(r) = e^{-jkr}/4\pi r$ defined above, the radiated pressure can be expressed under the form:

$$\begin{aligned} P(r,\theta) &= D_d \left(jk + \frac{1}{r}\right) G(r) \cos\theta \\ &= -D_d \frac{\partial G}{\partial r} \cos\theta \ . \end{aligned} \tag{12.39}$$

[6]Notice that some authors define $D_d = Ud$ as the moment of the dipole.

In the time-domain, the pressure is written:

$$p(r,\theta,t) = \frac{\cos\theta}{4\pi r}\left[\frac{1}{r}d_d\left(t-\frac{r}{c}\right) + \frac{1}{c}\frac{d}{dt}d_d\left(t-\frac{r}{c}\right)\right]. \tag{12.40}$$

The variable d_d has the dimension of an acceleration. The pressure here results from two terms: one acceleration term and another term proportional to the time derivative of the acceleration, which corresponds to a third-order time derivative. The contribution of this second term is dominant for the rapidly varying pressure, such as those resulting from percussive impacts, for example, for which instantaneous levels can reach very high values.

Applying the same method as for the sphere, we get the radial intensity:

$$I_r = \frac{1}{2}\rho c\left(\frac{k^2\,|U|\,d}{4\pi r}\right)^2 \cos^2\theta\ . \tag{12.41}$$

The other components of the intensity vector are zero. The power radiated by the dipole [a particular case of Eq. (12.28)] is

$$\mathscr{P}_r = \rho c\frac{k^4\,|U|^2\,d^2}{24\pi} = \rho\frac{\omega^4\,|U|^2\,d^2}{24\pi c^3}\ . \tag{12.42}$$

12.4.3.2 Second Approach

As done previously for the monopole, the pressure radiated by a dipole source is directly derived from the heterogeneous wave equation. For a particle oscillating with volume velocity U at constant volume between two positions r_1 and r_2, the fluid in this region is subjected to a force $f_0 = j\omega\rho U$, according to Newton's second law of motion (see Fig. 12.13). As a consequence, the spatial derivatives (the divergence term) yield the Dirac delta functions corresponding to the discontinuities of the force field in r_1 and r_2. The heterogeneous equation becomes

$$\frac{1}{c^2}\frac{\partial^2 p}{\partial t^2} - \Delta p = -\mathrm{div}\,\boldsymbol{f} = f_0\left[\delta(\boldsymbol{r}-\boldsymbol{r_1}) - \delta(\boldsymbol{r}-\boldsymbol{r_2})\right]. \tag{12.43}$$

In the frequency domain, taking advantage of the properties of the Green's function in free space in Eq. (12.20), we derive the pressure:

$$P(\boldsymbol{r}) = \frac{j\omega\rho U}{4\pi}\left[\frac{e^{-jk|\boldsymbol{r}-\boldsymbol{r_2}|}}{|\boldsymbol{r}-\boldsymbol{r_2}|} - \frac{e^{-jk|\boldsymbol{r}-\boldsymbol{r_1}|}}{|\boldsymbol{r}-\boldsymbol{r_1}|}\right]. \tag{12.44}$$

We find again the intuitive result obtained as the radius of the oscillating sphere tends to zero. This shows that the acoustic field generated by an elementary oscillating source is equivalent to the one radiated by two monopoles of identical

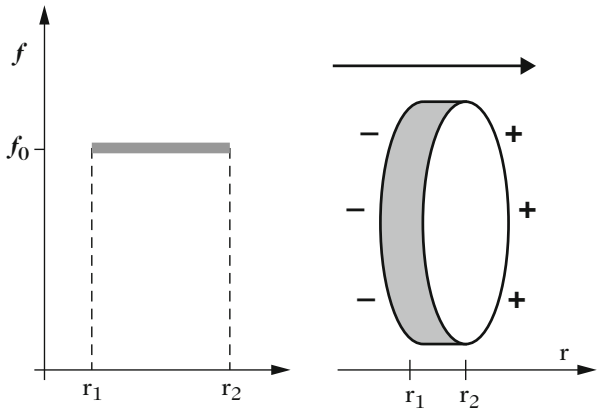

Fig. 12.13 Forces exerted on an elementary dipole

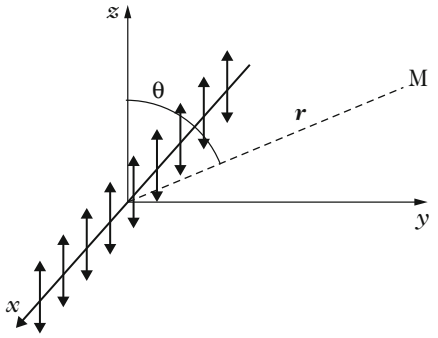

Fig. 12.14 Radiation of an isolated vibrating string. The string is stretched along the x-axis and is assumed to vibrate transversely along the z-axis. The oscillating string can thus be viewed as a linear array of dipoles oriented in the direction of the z-axis. The observation point M is located in the vertical plane, at a distance r from the string with an elevation angle θ with regard to the z-axis

volume velocity and opposite signs, where the distance between the point sources is determined by the peak-to-peak amplitude of the oscillation.

12.4.4 Distribution of Dipoles: Example of the Vibrating String

The vibrating string is a good example of a continuous distribution of dipoles. Before tackling in the next chapters the radiation of a complete stringed instrument, it is a interesting step to calculate the acoustic power radiated by an isolated string, not coupled to a soundboard. The examined configuration is shown in Fig. 12.14. The vector $\boldsymbol{D} = j\omega\rho U\boldsymbol{d}$ is the moment of the elementary dipoles oscillating along the z-axis and $\boldsymbol{d}$ is the vector oriented from $-U$ to $+U$. The pressure is calculated

at point M of coordinates (y, z) (or, alternatively, (r, θ)), with $r = \sqrt{y^2 + z^2}$ and $\cos\theta = y/r$. With $\boldsymbol{r}_1 = \boldsymbol{r}' - \boldsymbol{d}/2$ and $\boldsymbol{r}_2 = \boldsymbol{r}' + \boldsymbol{d}/2$ in (12.44), one obtains

$$P(\boldsymbol{r}) = \frac{j\omega\rho U}{4\pi}\left[\frac{e^{-jk|\boldsymbol{r}-\boldsymbol{r}'+\boldsymbol{d}/2|}}{|\boldsymbol{r}-\boldsymbol{r}'+\boldsymbol{d}/2|} - \frac{e^{-jk|\boldsymbol{r}-\boldsymbol{r}'-\boldsymbol{d}/2|}}{|\boldsymbol{r}-\boldsymbol{r}'-\boldsymbol{d}/2|}\right]. \tag{12.45}$$

If $|\boldsymbol{d}|$ tends to zero in the previous equation, we get

$$P(\boldsymbol{r}) = -j\omega\rho U\boldsymbol{d}.\mathbf{grad}\left[\frac{e^{-jk|\boldsymbol{r}-\boldsymbol{r}'|}}{4\pi\,|\boldsymbol{r}-\boldsymbol{r}'|}\right] = -\boldsymbol{D}.\mathbf{grad}\,[G(\boldsymbol{r}|\boldsymbol{r}')]\,. \tag{12.46}$$

One finds again the expression (12.39) obtained for an oscillating sphere whose radius tends to zero, and where θ is the angle between the vectors $\boldsymbol{D}$ and $(\boldsymbol{r} - \boldsymbol{r}')$.

Considering now the vibrating string as a linear distribution of dipoles yields the radiated pressure:

$$P(r) = -\frac{1}{4\pi}\frac{\partial}{\partial z}\left[\int_L D(x)\frac{e^{-jk\sqrt{r^2+x^2}}}{\sqrt{r^2+x^2}}\,dx\right]. \tag{12.47}$$

In this formula, $D(x)$ contains the information on the vibratory state of the string. In general, the integral in Eq. (12.47) cannot be solved analytically. However, in order to continue the calculation with the objective of highlighting some typical orders of magnitude for the radiation, two additional assumptions are made:

1. $D(x) = j\omega\rho U_0 d$; which corresponds to a uniform oscillation of the string with diameter d.
2. The string is of infinite length.

In this particular case, Eq. (12.47) becomes

$$P(r) = -\frac{j\omega\rho U_0 d}{4\pi}\frac{\partial}{\partial z}\left[\int_{-\infty}^{\infty}\frac{e^{-jkr\sqrt{1+w^2}}}{\sqrt{1+w^2}}\,dw\right], \tag{12.48}$$

with the change of variable $w = x/r$. It can be shown (see, for example, [31]) that the pressure is written:

$$P(r) = \frac{\rho c U_0 d}{4}\,k^2\,H_1^{(2)}(kr)\cos\theta, \tag{12.49}$$

where $H_1^{(2)}(kr)$ is the Hankel function of the second kind of order one[7] [2]. Another strategy for obtaining this result consists in solving the wave equation in cylindrical coordinates [20].

The acoustic power radiated per unit length of the string is derived from the calculations of pressure and acoustic velocity:

$$\mathscr{P}_r = \frac{\rho\omega^3 |U_0|^2 d^2}{16c^2} = \frac{\rho\pi^2\omega^3 |V_0|^2 d^4}{16c^2}, \tag{12.50}$$

where $U_0 = V_0 \pi dL$ with $L = 1$ m. V_0 is the oscillating velocity of the string. We can check on this expression that the radiated power varies as ω^3, which means that it increases rapidly with frequency. The strings of musical instruments generally have a small diameter (except for the low bass strings of the piano and of the double bass). According to Eq. (12.50), this means that they usually are very inefficient in terms of radiation. It is easy to make the experiment that the sound emitted by an isolated stretched string is almost inaudible, except if the string is put close to the ear.

12.4.5 Quadrupoles

Quadrupolar sources can be viewed as the association of dipoles. A few "musical" examples of such sources are presented below. The most common quadrupoles are the following:

- The *lateral* quadrupole whose plane configuration is shown in Fig. 12.15a. It corresponds to the association of four monopoles of alternate signs located at the corners of a square. The pressure radiated by this source in its plane is given by [14]:

$$P(r,\theta) = -j\rho c d^2 k^3 U \frac{e^{-jkr}}{4\pi r}\left[1 + \frac{3}{jkr} - \frac{3}{k^2 r^2}\right] \sin\theta\cos\theta\ . \tag{12.51}$$

  For a point situated outside its plane, the pressure is (see Fig. 12.16):

$$P(r,\theta,\phi) = -j\rho c d^2 k^3 U \frac{e^{-jkr}}{4\pi r}\left[1 + \frac{3}{jkr} - \frac{3}{k^2 r^2}\right] \sin\theta\cos\theta\ \cos\phi\ . \tag{12.52}$$

  The acoustic power radiated by the quadrupole is given by:

$$\mathscr{P}_r = \frac{\rho c d^4 k^6 |U|^2}{120\pi}\ . \tag{12.53}$$

[7] The Hankel functions of the first and second kind of order n are defined from the Bessel functions of the first kind J_n and from the Bessel functions of the second kind Y_n through the relation $H_n^{(1)}(z) = J_n(z) + jY_n(z)$ and $H_n^{(2)}(z) = J_n(z) - jY_n(z)$.

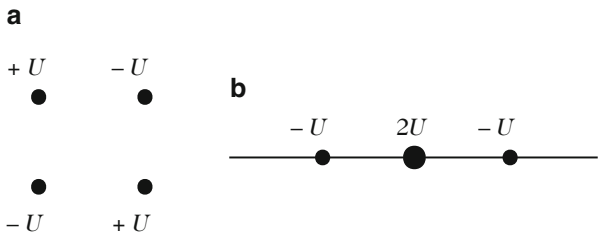

Fig. 12.15 (**a**) Lateral quadrupole. (**b**) Linear (or longitudinal) quadrupole

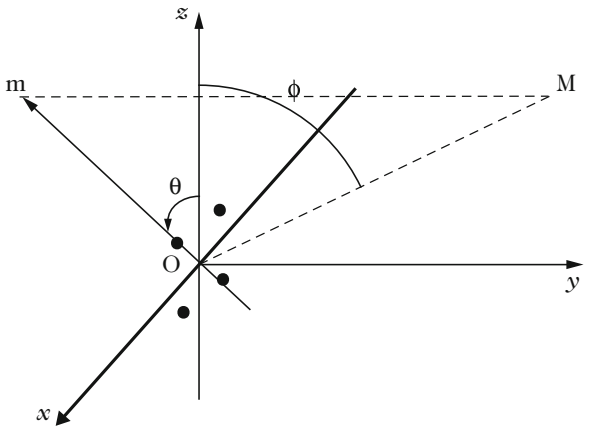

Fig. 12.16 Radiation of a lateral quadrupole: definition of the geometry outside the quadrupole plane. Point m is the projection of point M in the xOz-plane

This power is proportional to ω^6 which means that, for similar flow rate, this source is less efficient than a dipole in the low-frequency domain, though it increases more rapidly with frequency.

- The *linear (or longitudinal)* quadrupole, composed by two dipoles aligned on the same axis (see the Fig. 12.15b). The whole set is symmetrical with regard to the vertical plane, which yields a double flow rate $2U$ to the monopole in the center. In this case, the acoustic pressure is written [14]):

$$P(r,\theta) = -j\rho c d^2 k^3 U \frac{e^{-jkr}}{4\pi r}\left[\cos^2\theta\left(1+\frac{3}{jkr}-\frac{3}{k^2r^2}\right)-\frac{1}{jkr}+\frac{1}{k^2r^2}\right]. \tag{12.54}$$

Applying the same method as for the other elementary sources, the acoustic power of this quadrupole is derived:

$$\mathscr{P}_r = \frac{\rho c d^4 k^6 |U|^2}{40\pi}. \tag{12.55}$$

Compared to the lateral quadrupole, the same frequency dependence is observed (in ω^6). However, the resulting pressure (for identical flow rates) is three times higher.

12.4.5.1 Application 1: Acoustic Field Radiated by a Tuning Fork

The tuning fork is an essential device for each musician. We could have model this device as an example for illustrating the vibrations of beams in Chap. 1, but we prefer to focus here on its quadrupolar radiation properties. These properties were investigated by Russel [28]. In this study, the directivity of a tuning fork at a forced frequency around 440 Hz (note A4), and at different distances r from the source were investigated. The main results of this study are summarized below.

- At a frequency of 426 Hz (close to the nominal frequency of the fork) and at a distance $r = 5$ cm (close to the ear), we have $kr = 0.39$. On can thus reasonably consider to be in the near field. For this kr-value, it is not possible to derive from the simple observation of the directivity pattern whether the fork behaves as a lateral or as a longitudinal quadrupole, since both patterns are very similar (see Fig. 12.17). In both cases, four lobes are observed, which can be easily confirmed audibly by rotating the fork around its axis close to the ear. Notice, however, a

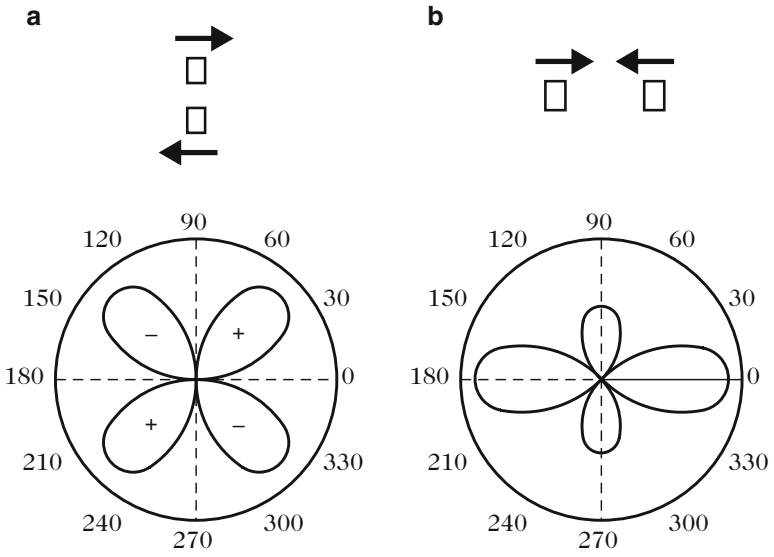

Fig. 12.17 θ- directivities of two quadrupoles for $kr = 0.39$. *Left*: (**a**) lateral quadrupole. *Right*: (**b**) longitudinal quadrupole [28]. The corresponding vibrational modes are displayed on top of each directivity pattern, as well as the motion of the tines. In the normal use of the fork, both branches vibrate at a nominal frequency of 440 Hz with the (**b**)-motion (note A4)

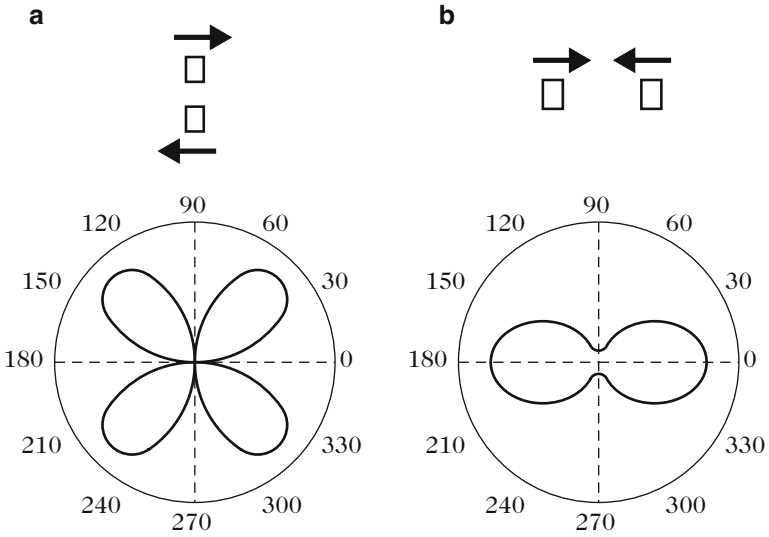

Fig. 12.18 Directivity along θ of quadrupoles for $kr = 7.8$. *Left*: lateral quadrupole. *Right*: longitudinal quadrupole. After [28]

difference of 5 dB between both models in the direction perpendicular to the axis of the fork [according to Eqs. (12.51) and (12.54)].

- If now the fork is located at a distance of 1 m from the ear ($kr = 7.8$), and slowly put into rotation around its axis, then only two maxima of the sound intensity are perceived for a complete turn, instead of four. In addition, the differences between the maximum and the minimum sound intensity level are less clearly audible than in the previous experiments. In this case, the directivity is clearly close to the one observed for the longitudinal quadrupole in the far field (see Fig. 12.18). This is coherent with the motion of the branches in the normal use of the fork.
- For $kr \gg 1$, the first-order approximation of Eq. (12.54) yields

$$P(r,\theta) \propto \frac{k^3}{r}\cos^2\theta \ . \tag{12.56}$$

This approximation accounts for the existence of two directivity lobes. However, this approximation predicts a zero amplitude in the axis perpendicular to the fork, which is neither in accordance with the complete model in Eq. (12.54), nor to the experiments.

In conclusion, these simple, and easy-to-reproduce, experiments illustrate the fact that the directivity of multipoles not only depend on frequency, but also on the distance of observation. In addition, it shows that oversimplified models can be not sufficient (and even wrong) for interpreting the experiments.

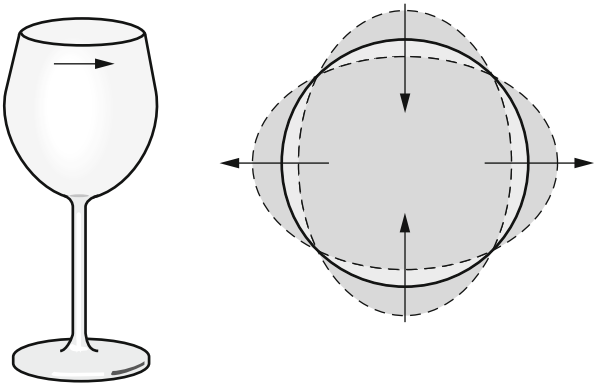

Fig. 12.19 Sliding the edge of a wine glass with a wet finger generates a self-sustained oscillation comparable to the one of a string excited by a bow. The glass vibrates close to a (2,0) mode (two nodal diameters) and the directivity of the sound field is similar to the one of a lateral quadrupole

12.4.5.2 Application 2: Radiation of Wine Glasses

Another easy to do experiments consists in sliding a wet finger on the edge of a glass. Several authors have shown that the main excited shell mode is of the $(2, 0)$-type (see Fig. 12.19). Such a mode is also often observed in the vibrations of bells [11, 27]. The excitation of this system involves typical stick-slip mechanisms, as for the bowed strings (see Chap. 11). Here, the sound is nearly a pure tone, since almost only one mode is strongly excited. The instrument called *glassharmonica* can be viewed as a generalization of this system. It has been used in the past by Mozart and other composers [4]. Figure 12.19 shows that the directivity of the sound field for this mode is analogous to the one of a lateral quadrupole, as verified experimentally by Russel [28].

12.5 Radiation of a Source with Arbitrary Shape

12.5.1 Kirchhoff–Helmholtz Integral

In this section, we are now dealing with the external field radiation of an extended acoustic source with arbitrary geometry, where a part of the external surface is subjected to a vibratory motion (see Fig. 12.20). This situation corresponds to the one encountered in most stringed and percussive instruments. Our purpose is to introduce a general formulation of the radiation, known as the Kirchhoff–Helmholtz integral. Except for very particular geometries, only numerical techniques (such as the Boundary Element Method, or BEM) can be used for solving such an integral (see Sect. 12.5.3.6 below). However, some approximations are valid, in some situations, leading to interesting results in terms of physics. Approximate

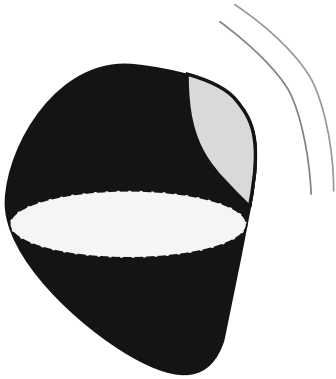

Fig. 12.20 In the most general case, an extended acoustic source is composed of both vibrating surfaces (*in grey*) and rigid parts (*in black*). The rigid parts reflect the waves emitted by the vibrating surfaces. The total resulting pressure field is the sum of the direct field radiated by the vibrating surfaces and the field reflected by the rigid passive surfaces

results can also serve as reference solutions when the purpose is to evaluate the pertinence and consistency of a numerical solution.

The pressure field radiated by an extended source such as the one shown in Fig. 12.20 is together due to the vibrating surfaces and to the waves reflected by the rigid parts. As a consequence, it will be shown that the whole source can be viewed equivalently as the association of a monopole and dipole distributions. This is one fundamental result of the Kirchhoff–Helmholtz integral. The existence of two distributions is a consequence of the fact that the Helmholtz equation itself is of the second order.

12.5.1.1 Green's Theorem

In order to introduce the Kirchhoff–Helmholtz equation, a mathematical tool is needed that allows the transformation of a volume integral into a surface integral: the Green's theorem. The interest of such a transformation will appear later, especially for the use of the integral in numerical applications.

Let us select two arbitrary functions G and Φ, assuming that these functions have the adequate properties of continuity and derivability for the problem. These functions are defined in a volume $\mathcal{V}$ bounded by a surface S with external normal vector $\boldsymbol{n}$. It can be shown that:

$$\int_{\mathcal{V}} [G\Delta\Phi - \Phi\Delta G]\, d\mathcal{V} = \int_{\mathcal{V}} \mathrm{div}\,[G\mathbf{grad}\Phi - \Phi\mathbf{gradG}]\, d\mathcal{V} = \int_S \left[G\frac{\partial\Phi}{\partial n} - \Phi\frac{\partial G}{\partial n}\right] dS\,. \tag{12.57}$$

The main interest of this theorem, which is nothing but a generalization of the divergence theorem, is the transformation of a volume integral into a surface integral, thus reducing by one the dimension of the problem. If both functions have the same impedance boundary condition on S (or on a part of S), the integral is equal to zero on this surface (or, on the considered part). Recall that the impedance is defined as the ratio between G and $\partial G/\partial n$.

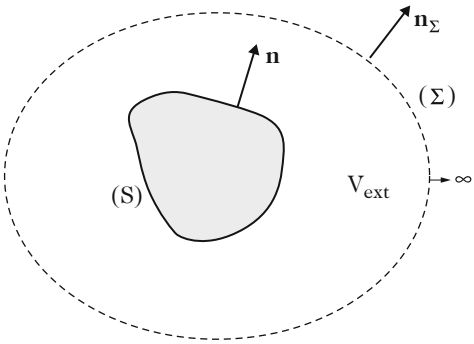

Fig. 12.21 Application of the Green's theorem to the calculation of the external pressure field

The application of the theorem (12.57) to the calculation of the external pressure field is illustrated in Fig. 12.21. The volume to consider here is the *external volume* denoted $\mathscr{V}_{\text{ext}}$ bounded by the external surface S of the source, on the one hand and, on the other hand, by the closed spherical surface Σ obtained as its radius tends to infinity:

$$\int_{\mathscr{V}_{\text{ext}}} [G\Delta\Phi - \Phi\Delta G]\, d\mathscr{V} = -\int_S \left[G\frac{\partial\Phi}{\partial n} - \Phi\frac{\partial G}{\partial n}\right] dS + \int_\Sigma \left[G\frac{\partial\Phi}{\partial n_\Sigma} - \Phi\frac{\partial G}{\partial n_\Sigma}\right] d\Sigma \,. \tag{12.58}$$

On Σ, the functions G and Φ fulfill the so-called *Sommerfeld condition* (see Sect. 12.5.1.2) and the integral vanishes. The change of sign in front of the first integral, in the right-hand side of the equation, is a consequence of the fact that the normal vector $\boldsymbol{n}$ is oriented towards the *internal part* of the volume $\mathscr{V}_{\text{ext}}$.

12.5.1.2 Calculation of the Pressure Radiated Outside the Source (External Field)

The purpose now is to determine the sound pressure $P(\boldsymbol{r})$ radiated by the acoustic source in the external field. This pressure is governed by the Helmholtz equation $\Delta P(\boldsymbol{r}) + k^2 P(\boldsymbol{r}) = 0$. In addition, the Green's function in free space is given by Eq. (12.20) where $\boldsymbol{r'}$ refers to any point on the surface S surrounding the volume $\mathscr{V}$ of the source. From these two equations, one can simply derive:

$$\Delta P(\boldsymbol{r})G(\boldsymbol{r}|\boldsymbol{r'}) - \Delta G(\boldsymbol{r}|\boldsymbol{r'})P(\boldsymbol{r}) = P(\boldsymbol{r})\delta(\boldsymbol{r} - \boldsymbol{r'}) \,. \tag{12.59}$$

Taking advantage of the reciprocity properties of the function G, Eq. (12.59) becomes

$$\Delta P(\boldsymbol{r'})G(\boldsymbol{r}|\boldsymbol{r'}) - \Delta G(\boldsymbol{r}|\boldsymbol{r'})P(\boldsymbol{r'}) = P(\boldsymbol{r'})\delta(\boldsymbol{r} - \boldsymbol{r'}) \,. \tag{12.60}$$

Finally, after integration over V_{ext} and application of the Green's theorem, we get

$$\int_{\mathscr{V}_{\text{ext}}} P(\mathbf{r}')\delta(\mathbf{r}|\mathbf{r}')d\mathscr{V} = P(\mathbf{r}) = \int_S \left[P(\mathbf{r}')\frac{\partial G(\mathbf{r}|\mathbf{r}')}{\partial n} - G(\mathbf{r}|\mathbf{r}')\frac{\partial P(\mathbf{r}')}{\partial n} \right] dS_{(\mathbf{r}')} \,. \tag{12.61}$$

The Kirchhoff–Helmholtz (KH) in (12.61) is valid for the *external* field. It shows that the pressure at any point $\boldsymbol{r}$ in the external space is obtained by means of a surface integral on the bounding surface S of the source.[8] This integral involves a distribution of monopoles (terms in $G(\boldsymbol{r}|\boldsymbol{r'})$), and a dipole distribution (terms in $\frac{\partial G(\boldsymbol{r}|\boldsymbol{r'})}{\partial n}$). In the following examples, the physical meaning of both distributions will be clarified.

Using Euler equation $\partial P/\partial n = -j\omega\rho V_n$, where V_n is the normal velocity (with regard to S), the KH-equation can be transformed into the following form[9]:

$$P(\boldsymbol{r}) = \int_S \left(-P(\boldsymbol{r'})\frac{e^{-jkR}}{4\pi R}\left[jk + \frac{1}{R} \right]\cos\theta + \frac{e^{-jkR}}{4\pi R} j\omega\rho V_n(\boldsymbol{r'}) \right) dS_{(\boldsymbol{r'})} \,. \tag{12.62}$$

Equation (12.62) shows that, for the calculation of the external pressure, knowledge of both the surface (parietal) pressure $P(\boldsymbol{r'})$ and normal velocity $V_n(\boldsymbol{r'})$ are necessary.

Sommerfeld Condition

In order to define a complete problem of radiation, initial and boundary conditions must be added to the partial differential (wave) equation. Writing in (12.58) that the integral on Σ vanishes as the observation distance tends to infinity corresponds to imposing a boundary condition at the infinity. In the far field ($r' \longrightarrow \infty$), we have $|\boldsymbol{r} - \boldsymbol{r'}| \simeq r'$. The integral then vanishes under the condition:

$$-4\pi r'^2 \left[P(\boldsymbol{r'})jk\frac{e^{-jk|\boldsymbol{r}-\boldsymbol{r'}|}}{4\pi r'} + \frac{e^{-jk|\boldsymbol{r}-\boldsymbol{r'}|}}{4\pi r'}\frac{\partial P(\boldsymbol{r'})}{\partial r'} \right] \to 0 \,. \tag{12.63}$$

Through permutation of r and r', this condition becomes

$$\lim_{r\to\infty} r\left[\frac{\partial P(r)}{\partial r} + jkP(r) \right] = 0 \,. \tag{12.64}$$

(continued)

[8] Notice that this integral is valid for any Green's function satisfying (12.20) in the external space, whatever the boundary conditions. In addition, this integral can be generalized to the case of multiple sources in the external space, due to the principle of superposition.

[9] It can be shown that the normal derivative of G is written $\frac{\partial G}{\partial n} = -G\left[jk + \frac{1}{R}\right]\cos\theta$, where $\theta = (\boldsymbol{n}, \boldsymbol{R})$.

This condition is the so-called *Sommerfeld condition*. Notice that the Green's function fulfills this condition. This amounts to assume that there is no convergent wave reflected back from infinity.

One drawback of the Sommerfeld condition is that it depends on the geometry. As a consequence, its exact formulation can be known explicitly only in a limited number of cases. An equivalent method for accounting to the zero condition at infinity is to consider that the wave is progressively damped during its propagation. This very "physical" method can be illustrated in the following 1-D case. Consider the transfer impedance [Eq. (4.29)]: if x_2 tends to infinity, the *tangent* function exhibits zeros and infinite maxima, and does not converge, which indicates the presence of reflected waves. However, if the wavenumber k becomes complex, and is written $k - j\alpha$, then the *tangent* function (of complex angle) tends to unity and the impedance tends to the characteristic impedance of a progressive wave, due to the absence of returning wave. In this case, the damping factor α can be imposed as small as we want. Finally, a Sommerfeld condition is obtained for the plane wave case: $\partial P/\partial x + jkP \longrightarrow 0$.

It will be shown in Chap. 14 that, for numerical necessity, another widely used method for simulating the radiation and propagation of waves in free space consists in imposing Absorbing Boundary Conditions at the border of a finite computational domain (such as a "virtual" anechoic chamber) in order to prevent the propagation of returning waves back to the source.

12.5.1.3 Time-Domain Formulation of the KH Integral

At this stage, a transformation of the KH integral in the time-domain can be achieved. The operator $j\omega$ corresponds to a time derivative, while $\exp(-jkr)$ corresponds to a time delay r/c. The pressure is then written:

$$p(\mathbf{r},t) = -\frac{1}{4\pi}\int_S \left[\frac{1}{Rc}\frac{\partial}{\partial t}p\left(\mathbf{r}', t-\frac{R}{c}\right) + \frac{1}{R^2}\,p\left(\mathbf{r}', t-\frac{R}{c}\right)\right]\cos\theta\; dS_{(\mathbf{r}')} + \frac{\rho_0}{4\pi}\int_S \frac{\partial v_n}{\partial t}\left(\mathbf{r}', t-\frac{R}{c}\right)\; dS_{(\mathbf{r}')}\,. \tag{12.65}$$

Equation (12.65) shows the *implicit* character of the equation, since the surface pressure p also appears under the integral. This induces some difficulties in the resolution. In addition, two terms are present in the first integral, where the magnitude of the second (in $1/R^2$) is attenuated more rapidly than the first one during the propagation. This first integral is of the dipolar type [see Eq. (12.40)]. The second integral is of the monopolar type, as in Eq. (12.14).

12.5.2 Multipolar Decomposition

Under the condition that the external surface S is sufficiently regular, it can be shown that the Kirchhoff–Helmholtz integral can be expanded as a convergent series of multipoles, whatever the size of the source. This approximation is particularly useful for the sources whose characteristic dimensions are small compared to the wavelength. Such a decomposition can be obtained using Taylor series expansion of vector functions f such as [2]:

$$f(\boldsymbol{r}-\boldsymbol{r}') = f(\boldsymbol{r}) - (\boldsymbol{r}'.\mathbf{grad})f(\boldsymbol{r}) + \frac{1}{2!}(\boldsymbol{r}'.\mathbf{grad})^2 f(\boldsymbol{r}) + \cdots \tag{12.66}$$

Applying this expansion to the function $R^{-1}p\,(\mathbf{r}', t - R/c)$, where $R = |\mathbf{r} - \mathbf{r}'|$, we get

$$\frac{p\,(\mathbf{r}', t-R/c)}{R} = \frac{1}{r}p\left(\mathbf{r}', t-R/c\right) - (\mathbf{r}'.\mathbf{grad})\frac{p\,(\mathbf{r}', t-R/c)}{r} + \frac{1}{2!}(\mathbf{r}'.\mathbf{grad})^2\frac{p\,(\mathbf{r}', t-R/c)}{r} + \cdots \tag{12.67}$$

or, equivalently:

$$\frac{p\left(\boldsymbol{r}', t-\frac{R}{c}\right)}{R} = \exp(-\boldsymbol{r}'.\mathbf{grad})\frac{p\left(\boldsymbol{r}', t-\frac{r}{c}\right)}{r} \quad \text{with}$$
$$\exp(-\boldsymbol{r}'.\mathbf{grad}) = 1 - \boldsymbol{r}'.\mathbf{grad} + \tfrac{1}{2!}(\boldsymbol{r}'.\mathbf{grad})^2 + \cdots . \tag{12.68}$$

Applying this result to both the pressure and velocity in (12.65), the KH integral is rewritten as follows:

$$p(\boldsymbol{r}, t) = -\tfrac{1}{4\pi}\int_S \exp(-\boldsymbol{r}'.\mathbf{grad})(\boldsymbol{n}.\mathbf{grad})\tfrac{p(\boldsymbol{r}', t-r/c)}{r}\, dS_{(\boldsymbol{r}')} + \tfrac{\rho}{4\pi r}\int_S \exp(-\boldsymbol{r}'.\mathbf{grad})\tfrac{\partial v_n}{\partial t}\,(\boldsymbol{r}', t-r/c)\; dS_{(\boldsymbol{r}')}\,. \tag{12.69}$$

Then, defining the following quantities:

$$\begin{cases} S(t) = \dfrac{\rho}{4\pi}\displaystyle\int_S \dot{v}_n(\boldsymbol{r}', t)\, dS, \\ \boldsymbol{D}(t) = \dfrac{1}{4\pi}\displaystyle\int_S \left[\rho\, \boldsymbol{r}'\, \dot{v}_n(\boldsymbol{r}', t) + \boldsymbol{n}\, p(\boldsymbol{r}', t)\right] dS, \\ Q_{ij}(t) = \dfrac{1}{8\pi}\displaystyle\int_S \left[\rho\, r'_i\, r'_j\, \dot{v}_n(\boldsymbol{r}', t) + (r'_i\, n_j + r'_j\, n_i)p(\boldsymbol{r}', t)\right] dS\,, \end{cases} \tag{12.70}$$

where the indices i and j refer to the vector components, the radiated pressure is expressed as follows:

$$p(r,t) = \frac{S(t-r/c)}{r} - \mathbf{grad}.\frac{\boldsymbol{D}(t-r/c)}{r} + \sum_{i,j=1}^{3} \frac{\partial^2}{\partial x_i \partial x_j}\frac{Q_{ij}(t-r/c)}{r} + \cdots . \tag{12.71}$$

In (12.71), $S(t)$ is the monopolar term, the vector $\boldsymbol{D}$ is the dipole moment, and the Q_{ij} are the quadrupolar components of the source.

12.5.2.1 Spherical Harmonics Expansion

The interest of the multipolar decomposition is to formulate the pressure field radiated by any source as a sum of elementary fields radiated by point sources of increasing order. However, from a mathematical point of view, such a decomposition might be problematic, because the selected basis is not orthogonal. For this reason, it is often preferred to expand the pressure on a spherical harmonics basis, which is orthogonal. For the external problem, and assuming no returning wave propagating towards the source, this expansion is written: [35]:

$$P(r,\theta,\phi,\omega) = \sum_{n=0}^{\infty} \sum_{m=-n}^{n} C_{mn}\, h_n(kr)\, Y_n^m(\theta,\phi), \tag{12.72}$$

where the C_{mn} are complex coefficients depending on frequency, the $h_n(kr)$ are *Spherical Hankel functions*[10], and the $Y_n^m(\theta,\phi)$ are the *spherical harmonics* [2]. These harmonics are written explicitly:

$$Y_n^m(\theta,\phi) = \sqrt{\frac{2n+1}{4\pi}\,\frac{(n-m)!}{(n+m)!}}\, P_n^m(\cos\theta)\; e^{jm\phi}, \tag{12.73}$$

where the P_n^m are the Legendre polynomials.

There is no bijection between the coefficients of the multipolar expansion and the spherical harmonics. However, it is relatively easy to express the first coefficients of the multipolar expansion in terms of spherical harmonics. The first spherical harmonic

$$Y_0^0(\theta,\phi) = \frac{1}{\sqrt{4\pi}} \tag{12.74}$$

[10]With the time convention selected throughout this book, the spherical Hankel functions here are of the second kind, defined as $h_n^{(2)}(z) = j_n(z) - jn_n(z)$, where $j_n(z)$ and $n_n(z)$ are the spherical Bessel functions of the first and second kinds, respectively. The exponent (2) is omitted for clarity.

for example, is a monopolar term. Similarly, the second spherical harmonic

$$Y_1^0(\theta,\phi) = \sqrt{\frac{3}{4\pi}}\cos\theta \tag{12.75}$$

has the directivity of an axial dipole . One can also show that the directivity of a longitudinal quadrupole can be derived from the difference $Y_2^0 - \alpha Y_0^0$ where α is a constant (see [35]).

Radiated Power

The acoustic power can be obtained through integration of the acoustic intensity on a sphere Σ of radius r_0 around the source. We obtain

$$\mathscr{P}_r(\omega) = \frac{1}{2}\int_\Sigma \Re e\left[P(r_0,\theta,\varphi,\omega)V^*(r_0,\theta,\varphi,\omega)\right] r_0^2 \sin\theta \; d\theta \; d\varphi \; . \tag{12.76}$$

Using Euler equation and the spherical harmonics expansion of the pressure, the acoustic velocity is written:

$$V(r_0,\theta,\varphi,\omega) = -\frac{1}{j\rho ck}\frac{\partial P}{\partial r} = -\frac{1}{j\rho c}\sum_{n=0}^{\infty}\sum_{m=-n}^{n} C_{mn}\, h_n'(kr_0)\; Y_n^m(\theta,\phi) \; . \tag{12.77}$$

The acoustic power can thus be rewritten as:

$$\mathscr{P}_r(\omega) = \frac{r_0^2}{2\rho c}\sum_{n=0}^{\infty}\sum_{m=-n}^{n} |C_{mn}^2| \Re e\left[h_n(kr_0)h_n'(kr_0)^*\right] \; . \tag{12.78}$$

Using one characteristic property of the spherical Hankel functions:

$$\Re e\left[h_n(kr_0)h_n'(kr_0)^*\right] = \frac{1}{k^2 r_0^2}, \tag{12.79}$$

it is found finally that the radiated power can be expressed in terms of the spherical harmonics under the form:

$$\mathscr{P}_r(\omega) = \frac{1}{2\rho ck^2}\sum_{n=0}^{\infty}\sum_{m=-n}^{n} |C_{mn}^2| \; . \tag{12.80}$$

This result shows that, due to their orthogonality property, the spherical harmonics are independent and thus the acoustic power radiated by each component only depends on the squared modulus $|C_{mn}|^2$ of its magnitude.

12.5.2.2 A Few Applications of the Spherical Harmonics in Musical Acoustics

Radiation of a Stringed Instrument with Holes

In the 1980s, Weinreich and Arnold have developed a new technique for measuring acoustic fields, based on the spherical harmonics expansion of the sound pressure. This technique was applied with success to the violin [34]. More precisely, Weinreich and his colleagues made the measurements of the *radiativities* of a stringed instrument, such as the violin, defined as the ratio between the so-called *multipolar moments* μ_{mn} and the force F_B exerted by the string at the bridge [33]. The moments defined by this author are related to the coefficients C_{mn} of the expansion in Eq. (12.72) by the relations[11]:

$$C_{mn} = \left[-j\omega\rho c \frac{k^{n+2}}{\sqrt{4\pi(2n+1)}} \frac{2^n n!}{(2n)!} \right] \mu_{mn} \,. \tag{12.81}$$

With this definition, one can show that the moments μ_{mn} for a sphere of radius a small compared to the wavelength ($ka \ll 1$) and subjected to a radial motion $\xi(r = a, \theta, \varphi)$ are given by:

$$\mu_{mn} = \frac{4\pi\sqrt{2n+1}a^{n+2}}{n+1} \int_{\varphi=0}^{2\pi} \int_{\theta=0}^{\pi} Y_n^{m*}(\theta, \varphi)\, \xi(a, \theta, \varphi) \sin\theta \, d\theta \, d\varphi, \tag{12.82}$$

due to the orthogonality properties of the spherical harmonics [35]. One can check, in particular, that for $m = n = 0$, the monopolar moment is written:

$$\mu_{00} = \int_{\varphi=0}^{2\pi} \int_{\theta=0}^{\pi} \xi(a, \theta, \varphi)\, a^2 \, \sin\theta \, d\theta \, d\varphi, \tag{12.83}$$

which corresponds to the volume variation of the sphere during its motion.

One interest of the spherical harmonics expansion is due to its rapid convergence as the order n becomes higher than ka, where a is a characteristic dimension of the source. Keeping a few terms only in the expansion (12.72) is then sufficient for obtaining a good estimate of the radiated field. Assuming a characteristic dimension of the order of 10 cm for the violin, for example, then an expansion up to the second order yields a good approximation of the radiated field between 0 and 1 kHz.

The radiativities $\Gamma_{mn} = \mu_{mn}/F_B$ are functions of frequency which can be further expanded on the eigenmodes basis (see Part II of this book):

[11] This definition by the author of the acoustic multipolar moments is dictated by analogies with corresponding definitions in electrodynamics. Let us also mention that, in the presently cited paper, the index n is replaced by the index l and the order of the indices is reversed. As a consequence, the moment μ_{mn} defined here corresponds to the moment μ_{lm} in Weinreich's paper.

$$\Gamma_{mn}(\omega) = \sum_j \frac{A^j_{mn}}{\omega - \omega_j}, \tag{12.84}$$

where the ω_j are the complex eigenfrequencies of the source (see Sect. 2.2.1 in Chap. 2), and where the A^j_{mn} are also complex constants. This expression is also written:

$$-\Gamma_{mn}(\omega) = \sum_j \frac{A^j_{mn}}{\omega_j} + \omega \sum_j \frac{A^j_{mn}}{\omega_j^2} + \omega^2 \sum_j \frac{A^j_{mn}}{\omega_j^3} + \cdots . \tag{12.85}$$

- *Back to the physics of the violin*. For $\omega \to 0$, the behavior of the instrument in *quasi-static* regime is obtained. This corresponds to very low frequencies, where the air can be considered as incompressible. In other words, applying a vertical force F_B on the soundboard, then the decrease in air volume inside the box is exactly compensated by the volume of air escaping through the f-holes. As a consequence, Eq. (12.83) indicates that the monopolar moment μ_{00} must be zero, which implies

$$\sum_j \frac{A^j_{00}}{\omega_j} = 0 . \tag{12.86}$$

This result is valid for any musical instrument made of a vibrating shell with holes (guitar, lute,...). It is the so-called *sound hole sum rule*.

Neglecting the damping terms yields real eigenfrequencies. In this case, the radiativities become

$$\Gamma_{mn}(\omega) \simeq \sum_j \frac{B^j_{mn}}{\omega^2 - \omega_j^2}. \tag{12.87}$$

These expressions can be expanded as follows[12]:

$$-\Gamma_{mn}(\omega) \simeq \sum_j \frac{B^j_{mn}}{\omega_j} + \omega^2 \sum_j \frac{B^j_{mn}}{\omega_j^3} + \omega^4 \sum_j \frac{B^j_{mn}}{\omega_j^5} + \cdots . \tag{12.88}$$

It can be seen that the terms of odd exponent in ω are not present in the expansion (12.88). As mentioned earlier, the constant term vanishes, because of the

[12]The coefficients in the numerator are denoted B^j_{mn}, in order to make the difference with the coefficients A^j_{mn}. We do not write the relationships between these two families of coefficients explicitly, since it is not necessary for the present demonstration.

sound hole sum rule. The first nonzero term is in ω^2, which corresponds to a dipole (see, for example, Eq. (12.39). As a consequence, the radiated power is proportional to ω^4.

For stringed instruments such as the violin or the guitar, the modal damping coefficients ζ_j (see the definition of these coefficients in Eq. (2.3)) generally are in average smaller than 0.05 below the lowest mode, so that the approximation (12.88) is justified. One can conclude that these instruments radiate as dipoles below the first mode.

Virtual Sources

The reproduction of the acoustic field radiated by a given source is another growing application of the spherical harmonics. In the music world, the use of synthesizers and electronic amplification leads to the question of sound diffusion through loudspeakers. In fact, recording a given instrument (flute, or violin,...) and reproducing it through a standard stereophonic apparatus composed of 3-way loudspeaker systems, then there is very little probability that the reproduced sound field will be identical to the one radiated by the original recorded instrument. Even if the human ear recognizes the type of instrument without ambiguity, the directivity of the source (and, even, its timbre) might be substantially altered by the electroacoustic system.

For many years, the research team at IRCAM (Institut de Recherche et Coordination Acoustique-Musique) in Paris have tackled that question [8]. Here again, they took advantage of the fast convergence of the spherical harmonics expansion for approximating real sources with an array of loudspeakers. The first step of the method consists in measuring the directivity $\mathscr{D}$ of a given instrument (violin and upright piano) in free field (anechoic chamber) at a given distance from the instrument, and for different frequencies. The measured directivity pattern is then decomposed on a truncated spherical harmonics basis. To a first approximation, this truncated basis contains the monopolar component and the three dipole components. This can be written formally:

$$\mathscr{D} \simeq a_1 \mathscr{D}_m + a_2 \mathscr{D}_{d1} + a_3 \mathscr{D}_{d2} + a_4 \mathscr{D}_{d3}, \tag{12.89}$$

where the $a_i(\omega)$ are the unknowns of the problem. These coefficients (or filters) can be estimated by using, for example, least square methods where the goal is to minimize the distance between measured and approximate directivity.

As soon as the filters $a_i(\omega)$ are determined, the recorded sound is played through loudspeaker arrays, where each group of loudspeakers has been first designed so that its directivity pattern corresponds either to a monopole or to one of the three dipoleterms, with one dipole oriented in each of the three directions of the coordinates. In summary, the principles of the diffusion is shown in Fig. 12.22. The recorded signal is filtered in parallel on the i channels of the expansion. The output

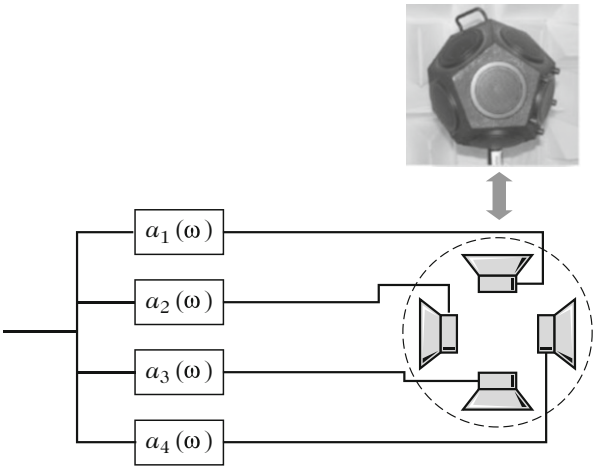

Fig. 12.22 This figure shows the basic principles of sound reproduction of a given instrument (piano and violin) by a loudspeaker array (here, a dodecahedron), so that the array has a directivity similar (or close) to the one of the real instrument. For this purpose, the sound radiated by the instrument is recorded and fed into a filter bank $a_i(\omega)$. The output signal of each filter is, in turn, fed into groups of loudspeakers, where each group has either the directivity of a monopole or the one of a dipole. The sum of all output pressure patterns must fulfills the condition (12.89), which corresponds to the directivity of the real instrument. After [8]

of each filter a_i is fed into the loudspeaker array corresponding to its directivity. The whole set of loudspeakers is usually grouped into a single extended source (cube, dodecahedron, ...).

12.5.3 Radiation of Sound in a Semi-Infinite Space

12.5.3.1 General Formulation

In the previous sections, it has been shown to what extent the acoustic pressure that reaches the ear of a listener depends on the velocity profile of the external surface of the source, and on its geometry. It has been also pointed out that the passive surfaces (without sources) contribute to the radiation field. This last property is generalized here where it is shown that the sound field is influenced by the passive surfaces situated in the vicinity of the sources. The acoustic field radiated by a loudspeaker located in the corner of a room, for example, is not the same as the one resulting from the same loudspeaker (playing the same sound) located in the center of the room. Similarly, recording an instrument (a cello, for example) in a room with a very reflective floor can be surprising! In this case, the sound that reaches the microphone is

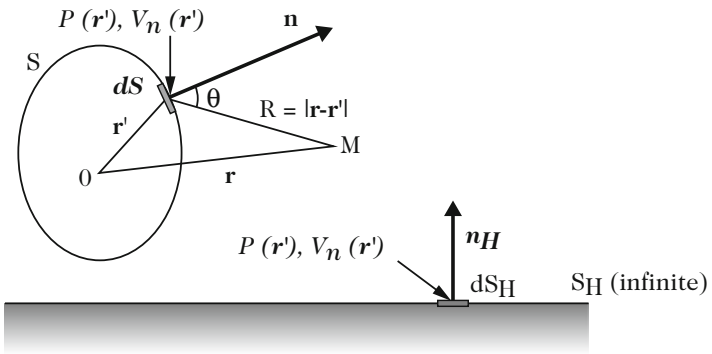

Fig. 12.23 Source in the vicinity of an infinite plane

the sum of the direct field and the field reflected by the floor. Constructive (or destructive) interferences can result from this superposition which might alter the timbre of the instrument substantially, like the well-known "comb-filter" effect. In order to address this question, we consider the simple situation, shown in Fig. 12.23 where the source is situated in the vicinity of an infinite plane S_H with normal vector $\boldsymbol{n_H}$.

As for S, $\boldsymbol{r'}$ denotes any point of S_H, where the pressure and the acoustic velocity are denoted $P(\boldsymbol{r'})$ and $V_n(\boldsymbol{r'})$, respectively. According to the superposition theorem, Eq. (12.61) becomes

$$P(\boldsymbol{r}) = \int_S \left[P(\boldsymbol{r'}) \frac{\partial G(\boldsymbol{r}|\boldsymbol{r'})}{\partial n} - G(\boldsymbol{r}|\boldsymbol{r'}) \frac{\partial P(\boldsymbol{r'})}{\partial n} \right] dS + \int_{S_H} \left[P(\boldsymbol{r'}) \frac{\partial G(\boldsymbol{r}|\boldsymbol{r'})}{\partial n_H} - G(\boldsymbol{r}|\boldsymbol{r'}) \frac{\partial P(\boldsymbol{r'})}{\partial n_H} \right] dS \,. \tag{12.90}$$

12.5.3.2 Particular Case: Half-Space Delimited by an Infinite Rigid Plane

In the particular case where an infinite plane delimiting the half-space is supposed to be rigid, then the velocity normal to this plane is supposed to be zero. Equation (12.90) can be simplified through the use of a new Green's function G_H which takes the presence of the rigid plane into account. In other words, a function $G_H(\boldsymbol{r}|\boldsymbol{r'})$ is searched which fulfills both the Sommerfeld condition and the boundary condition $V_n = 0$ on S_H. We have

$$\Delta G_H(\boldsymbol{r}|\boldsymbol{r'}) + k^2 G_H(\boldsymbol{r}|\boldsymbol{r'}) = -\delta(\boldsymbol{r}|\boldsymbol{r'}) \;\text{ with }\; \left.\frac{\partial G_H}{\partial n_H}\right|_{S_H} = 0 \,. \tag{12.91}$$

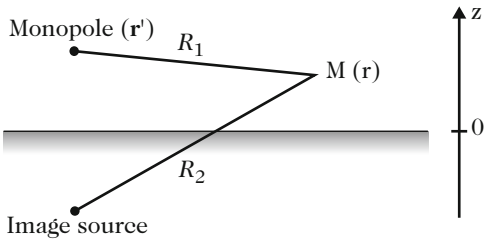

Fig. 12.24 Green's function for an half-space bounded by an infinite plane

It can be easily checked that the function:

$$G_H(\boldsymbol{r}|\boldsymbol{r'}) = \frac{e^{-jkR_1}}{4\pi R_1} + \frac{e^{-jkR_2}}{4\pi R_2}, \tag{12.92}$$

where R_1 and R_2 are the distances defined in Fig. 12.24, fulfills the required conditions of the problem.

In Cartesian coordinates, these distances are given by:

$$\begin{aligned} R_1 &= \left[(x-x')^2 + (y-y')^2 + (z-z')^2\right]^{1/2} \\ R_2 &= \left[(x-x')^2 + (y-y')^2 + (z+z')^2\right]^{1/2}, \end{aligned} \tag{12.93}$$

where R_1 is the distance between one point source and the observation point, and R_2 is the distance between the image of the source point (with regard to the plane S_H) and the observation point.

On S_H, or equivalently for $z = 0$, we have $R_1 = R_2 = R$ and $\frac{\partial R_1}{\partial z} + \frac{\partial R_2}{\partial z} = 0$. As a consequence, the expression (12.92) fulfills

$$\left.\frac{\partial G_H}{\partial n_H}\right|_{S_H} = \left.\frac{\partial G_H}{\partial z}\right|_{S_H} = 0\,. \tag{12.94}$$

Finally, G_H is obtained when the observation point $M(\boldsymbol{r})$ tends to the plane S_H, and is equal to:

$$G_{HS_H} = 2\frac{e^{-jkR}}{4\pi R} = 2G\,. \tag{12.95}$$

12.5.3.3 Radiation of a Plane Source Fixed in an Infinite Rigid Plane

The determination of the acoustic field is highly simplified in the particular case of the plane sources, especially in the far field. In this case, and under certain conditions, the implicit Kirchhoff–Helmholtz integral is transformed into the simpler explicit Rayleigh integral where the free-field pressure is derived from the velocity profile of the emitting surface.

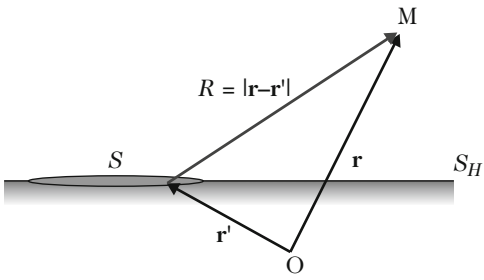

Fig. 12.25 Plane source of surface S fixed in an infinite rigid plane (S_H). The origin O is arbitrary. $\boldsymbol{r}$ is the coordinate vector of the observation point M. $\boldsymbol{r}'$ is the coordinate vector of a point on the source S

In musical acoustics, the Rayleigh integral is a convenient tool for computing, for example, the sound field radiated by a plane soundboard, to a first approximation. However, in this case, the condition of fixation in an infinite plane is not fulfilled, which leads to significant discrepancies with measurements, especially in the low-frequency range, when the acoustic wavelength is larger than the dimensions of the soundboard. The Rayleigh integral also yields wrong results in the soundboard plane and behind the source. Therefore, most precise predictive calculations applicable to real instruments will be presented in Chap. 13.

In this section, the main results for the radiation of a plane source fixed in an infinite rigid plane are briefly reviewed. More details can be found in many textbooks.

12.5.3.4 Rayleigh Integral

We consider an extended plane source with surface S fixed in an infinite rigid plane S_H (Fig. 12.25). It has been shown above that the Eq. (12.61) remains valid for any Green's function whatever the boundary conditions. We derive

$$P(\boldsymbol{r}) = \int_{S_H} \left[P(\boldsymbol{r}') \frac{\partial G_H}{\partial n_H} - G_H \frac{\partial P(\boldsymbol{r}')}{\partial n_H} \right] dS_H, \tag{12.96}$$

By definition, the normal derivative of the Green's function G_H is zero on the surface S_H. The normal derivative of the pressure $P(\boldsymbol{r})$ is also zero on S_H, except on S. We get

$$P(\boldsymbol{r}) = -\int_S G_H \frac{\partial P(\boldsymbol{r}')}{\partial n_H} dS\,. \tag{12.97}$$

Writing G_H explicitly [Eq. (12.95)], and using Euler equation, we get

$$P(\mathbf{r}) = \frac{j\omega\rho}{2\pi} \int_S \frac{V_n(\mathbf{r}')}{R}\, e^{-jkR}\, dS. \tag{12.98}$$

This last expression is the so-called *Rayleigh integral*.

12.5.3.5 Fresnel and Fraunhofer Approximations

For $|\boldsymbol{r}| \gg |\boldsymbol{r'}|$, it is useful to look for approximations of the Rayleigh integral, based on Taylor series expansion of R, as follows:

$$R = |\boldsymbol{r} - \boldsymbol{r'}| \simeq r - \boldsymbol{r'}.\boldsymbol{m} + \frac{1}{2r}\left[r'^2 - \left(\boldsymbol{r'}.\boldsymbol{m}\right)^2\right] + \cdots , \tag{12.99}$$

where $\boldsymbol{m}$ is the unitary vector $\boldsymbol{r}/r$.

In the so-called *Fraunhofer* approximation, the expansion (12.99) is truncated to the first two terms. As a consequence, the Rayleigh integral becomes

$$P(\boldsymbol{r}) \simeq \frac{j\omega\rho}{2\pi}\,\frac{e^{-jkr}}{r}\int_S V_n(\boldsymbol{r'})e^{-j\boldsymbol{k}.\boldsymbol{r'}}\,dS, \tag{12.100}$$

where $\boldsymbol{k} = k\boldsymbol{m}$. By definition, the spatial Fourier transform of $V_n(\boldsymbol{r'})$ is

$$\tilde{V}_n(\boldsymbol{k}) = \int_S V_n(\boldsymbol{r'})e^{-j\boldsymbol{k}.\boldsymbol{r'}}\,dS\,. \tag{12.101}$$

Finally, we get for the pressure:

$$P(\boldsymbol{r}) \simeq \frac{j\omega\rho}{2\pi}\,\frac{e^{-jkr}}{r}\,\tilde{V}_n(\boldsymbol{k}). \tag{12.102}$$

This result means that the magnitude of the pressure, besides the $1/r$ dependence, is fully determined by the *spatial Fourier transform* of the normal velocity field of the baffled source. Under the condition of adequate spatial discretization, this property opens a wide range of efficient methods for the calculation of radiated field, in view of the existence of numerous fast algorithms dedicated to the computation of discrete Fourier transforms.

In the *Fresnel* approximation, the first three terms of the expansion of R are kept. It is further assumed that the observation point is not too far from the x-axis or, equivalently, $r \simeq x$ (see Fig. 12.26). We can then calculate the acoustic field near the plane source and close to its axis. We have

$$R = |\boldsymbol{r} - \boldsymbol{r'}| \simeq x - \boldsymbol{m}.\boldsymbol{r'} + \frac{r'^2}{2x}\,. \tag{12.103}$$

Using the same notations as previously, the pressure is written:

$$P(\boldsymbol{r}) \simeq \frac{j\omega\rho}{2\pi}\,\frac{e^{-jkx}}{x}\int_S V_n(\boldsymbol{r'})e^{-j\boldsymbol{k}.\boldsymbol{r'}}\,e^{-\frac{jkr'^2}{2x}}\,dS\,. \tag{12.104}$$

This last expression also involves a Fourier transform. However, in the Fresnel case, the velocity field on the source has to be first multiplied by a phase factor. Denoting

V_{pn} this weighted velocity, we have:

$$V_{pn} = V_n(\boldsymbol{r'})\, e^{-\frac{jkr'^2}{2x}}, \tag{12.105}$$

and the acoustic pressure becomes

$$P(\boldsymbol{r}) \simeq \frac{j\omega\rho}{2\pi}\,\frac{e^{-jkr}}{r}\,\tilde{V}_{pn}(\boldsymbol{k})\ . \tag{12.106}$$

It can be shown that the limit between the Fresnel and the Fraunhofer zone is located at position $x = L^2/4\lambda \simeq L^2 f/4c$, where L is a characteristic dimension of the source, and λ the acoustic wavelength. This is an alternative way to define a limit between near and far field.

12.5.3.6 Source with Uniform Velocity Distribution, or "Plane Piston"

In this paragraph, the radiation of a plane circular disk of radius a subjected to a uniform velocity V_0 at frequency ω is considered. This well-known example is often called a "plane piston" (see Fig. 12.26). In the far field, it is assumed that the Fraunhofer approximation is valid, so that the pressure can be computed using (12.102). For the velocity, we have

$$V_n(r') = \begin{cases} V_0 \ \text{ for } \ 0 \le r' \le a, \\ 0 \ \text{ elsewhere}\ . \end{cases} \tag{12.107}$$

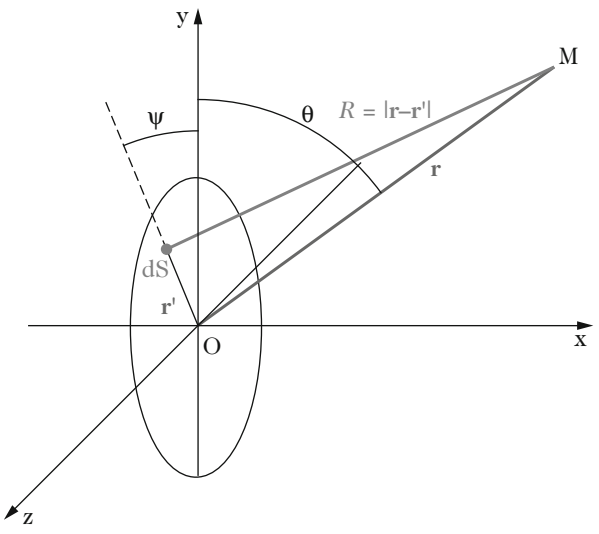

Fig. 12.26 Geometry of the plane piston. The circular disk of radius a is situated in the plane yOz and subjected to a uniform velocity V_0 oriented along the Ox-axis

As a consequence, its spatial Fourier transform is written:

$$\tilde{V}_n(\boldsymbol{k}) = U_0 \left[\frac{2J_1(ka\cos\theta)}{ka\cos\theta} \right] \tag{12.108}$$

where θ is the angle between the vector $\boldsymbol{r}$ and the source plane (see Fig. 12.26), and $U_0 = \pi a^2 V_0$ the volume velocity of the piston. The quantity $\mathscr{D}(\theta) = \frac{2J_1(ka\cos\theta)}{ka\cos\theta}$ is the *directivity* of the piston. The radiated pressure is written:

$$P(r,\theta) = \frac{j\omega\rho U_0}{2\pi} \frac{e^{-jkr}}{r} \mathscr{D}(\theta) \,. \tag{12.109}$$

Comparing this result with the pressure field radiated by a pulsating half-sphere shows that the directivity is more pronounced for an extended source than for a point source. The directivity increases with frequency. This general result can be explained as follows: at low frequencies, the different vibrating points of the surface S yield constructive interferences, whereas, with increasing frequency, the phase shifts due to the differences in the propagation distances at a given point in space are more and more pronounced, leading to destructive interferences, especially off-axis. The power radiated by the piston is equal to:

$$\mathscr{P}_r = \frac{\rho c k^2 |U_0|^2}{4\pi}, \tag{12.110}$$

which corresponds exactly to twice the sound power radiated by a monopole with identical volume velocity.[13] As a consequence of the source extension, the sound intensity is not distributed equally in all directions.

One interesting result for the circular plane piston is the calculation of the pressure on the axis since, in this particular case, an exact calculation of the pressure can be made without assuming a far field approximation. Figure 12.27 shows some examples for different values of the source radius a at various frequencies. At a frequency of 5.525 kHz and for a radius $a = 25$ cm, for example, it can be seen that the limit between near and far field is close to 1 m. below this limit, in the vicinity of the piston, the pressure shows rapid fluctuations. These fluctuations are reduced for a smaller radius, and at lower frequencies. Such properties are important to know when recording sound sources in general (including musical instruments), since the recorded signal is highly sensitive to the location of the microphone in the near field.

[13] This is due to the fact that the plane piston radiates in an half-space: the volume velocity in the complete space is $U_0' = 2U_0$, thus, expressing the power in (12.110) as a function of U_0' yields a factor 16 in the denominator. The total power in the two half-spaces is the sum of the power on each side of the rigid plane, and we find as a result the factor 8 in the denominator as in (12.21).

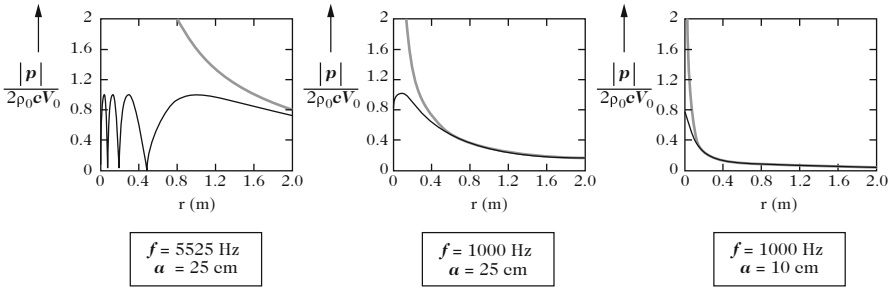

Fig. 12.27 Axial pressure field of a circular plane piston for different values of the radius a and oscillation frequency f. Comparison with the results obtained for a semi-monopole (in *grey color*). As a and f increase, more and more important amplitude fluctuations are seen in the vicinity of the piston. The monopole approximation becomes more and more relevant as both a and f decrease. However, this approximation is never realistic on the piston itself, since it predicts an infinite pressure

Boundary Element Method (BEM)

The Kirchhoff–Helmholtz (KH) integral forms the theoretical basis of the numerical *BEM: Boundary Element Method*. It mains attracting aspect lies in the fact that the KH integral is a surface integral (and not a volume integral) which contributes to reduce the computational burden substantially. In musical acoustics, this method has been applied to the guitar by Brooke [3] and Fleischer [32]. This last author also applied the BEM method to timpani. The main principles and difficulties of this method are briefly summarized below. The reader may consult specialized textbooks on this topic for more information [36].

In Eq. (12.61), the expression of $P(\boldsymbol{r})$ was given for an observation point situated in free space outside the external bounding surface S of the source. For an observation point situated on the surface S, one can show that the equation becomes

$$\frac{1}{2}P(\boldsymbol{r}) = \int_S \left[P(\boldsymbol{r}') \frac{\partial G(\boldsymbol{r}|\boldsymbol{r}')}{\partial n} - G(\boldsymbol{r}|\boldsymbol{r}') \frac{\partial P(\boldsymbol{r}')}{\partial n} \right] dS_{(\boldsymbol{r}')} \,. \tag{12.111}$$

The physical meaning of the factor $1/2$ can be explained by the fact that, on the surface, we have to define a Green's function in 2π steradians, and not in 4π steradians. The use is to group (12.61) and (12.111) in a single expression:

(continued)

$$\int_S \left[P(\boldsymbol{r}') \frac{\partial G(\boldsymbol{r}|\boldsymbol{r}')}{\partial n} - G(\boldsymbol{r}|\boldsymbol{r}') \frac{\partial P(\boldsymbol{r}')}{\partial n} \right] dS_{(\boldsymbol{r}')} = \epsilon P(\boldsymbol{r}) \quad \text{with} \quad \begin{cases} \epsilon = 1 \ \text{ for } \ M \in V_{\text{ext}}, \\ \epsilon = \dfrac{1}{2} \ \text{ for } \ M \in S \, . \end{cases} \tag{12.112}$$

The first level of approximation of the BEM method is of the *geometrical* type. It is due to the fact that the discretization of (12.112) requires a subdivision of the surface (or boundary) S in a number N_e of finite elements, so that:

$$\sum_{j=1}^{N_e} S_j \simeq S \, . \tag{12.113}$$

In (12.113), the symbol "$\simeq$" means that some fine details of the edges, and/or of the curvature of the surface, cannot be taken into account by such a discretization. Equation (12.112) becomes

$$\epsilon P(\boldsymbol{r}) = \sum_{j=1}^{N_e} \int_{S_j} \left[P(\boldsymbol{r}') \frac{\partial G(\boldsymbol{r}|\boldsymbol{r}')}{\partial n} - G(\boldsymbol{r}|\boldsymbol{r}') \frac{\partial P(\boldsymbol{r}')}{\partial n} \right] dS_{(\boldsymbol{r}')} \, . \tag{12.114}$$

For approximating the surface, one can use simple elements, such as triangles, or other geometrical forms of higher order (spline functions). The degree of accuracy of the approximation increases with the number of elements N_e and with the order of the surface elements.

The second level of approximation in the BEM method is of the *functional* type. This level govern how the variables P and G inside a given surface element are expressed as functions of their values in a number of fixed points called *nodes*. In the simplest case, it is assumed that these variables are approximated by piecewise constant functions. In this case, Eq. (12.114) is written:

$$\epsilon P(\boldsymbol{r}) = \sum_{j=1}^{N_e} P(r'_j) \int_{S_j} \frac{\partial G(\boldsymbol{r}|r'_j)}{\partial n} dS_{(\boldsymbol{r}')} - \sum_{j=1}^{N_e} \frac{\partial P(r'_j)}{\partial n} \int_{S_j} G(\boldsymbol{r}|r'_j) dS_{(\boldsymbol{r}')}, \tag{12.115}$$

and the number of nodes is equal to the number of elements. The expression of the pressure at points r_i becomes

$$\epsilon P(r_i) = \sum_{j=1}^{N_e} P(r'_j) M_{ij} - \sum_{j=1}^{N_e} \frac{\partial P(r'_j)}{\partial n} L_{ij} \tag{12.116}$$

(continued)

or, equivalently, in matrix form:

$$\epsilon \boldsymbol{P} = \mathbb{M}\, \boldsymbol{P}_S - \mathbb{L}\, \frac{\partial \boldsymbol{P}_S}{\partial n}\,. \tag{12.117}$$

In general, the normal velocity is a given parameter, so that $\frac{\partial \boldsymbol{P}_S}{\partial n}$ is known. The unknowns are $\boldsymbol{P}$ in free space and $\boldsymbol{P}_S$ on the surface S. In a first step, it is necessary to determine $\boldsymbol{P}_S$ in order to solve Eq. (12.117). This quantity is obtained as the observation point converges to the surface S, which means that $\boldsymbol{r}$ tends to $\boldsymbol{r}'$. Equation (12.117) becomes

$$[\mathbb{M} - \epsilon \mathbb{I}]\ \boldsymbol{P}_S = \mathbb{L}\, \frac{\partial \boldsymbol{P}_S}{\partial n}, \tag{12.118}$$

where $\mathbb{I}$ is the identity matrix. At this stage, one of the main difficulties of the BEM method is a consequence of the non-uniqueness of the solution observed for the eigenvalues of the operator $[\mathbb{M} - \epsilon \mathbb{I}]$. A physical meaning for this eigenvalues is difficult to find, since they result from a purely mathematical singularity problem. Some methods exist today, such as the *CHIEF* (or *Combined Helmholtz Integral Equation Formulation*), for overcoming such difficulties [32]: this last method is based on the idea to formulate (12.118) in the form of a overdetermined system which is solved by means of a least square method.

12.6 Radiation of Sound Tubes

The complexity of the radiation by wind instruments is mainly due to the existence of orifices, which can be large compared to the wavelength for brass instruments or saxophones. Moreover for woodwinds they can have a significant external interaction. Hereafter we give the main elements (i.e., the radiation impedance, which represents the effect inside the tube, and directivity of the radiated field outside) for the end of a tube, and we explain the principle of the interaction of two orifices. The radiation of instruments with several sources will be investigated in Chap. 14.

12.6.1 Radiation Impedances

12.6.1.1 First Approach

In what follows we consider the radiation by tubes without mean flow, in the linear approximation. An analysis of the flow influence can be found in the literature [6, 21, 24], and the issue of high levels is treated in Chap. 8 (Sect. 8.4.5) of the present book. Moreover we consider low Helmholtz number ka, where a is the tube radius, when only the planar mode propagates.[14] Results concerning non-planar modes of the tube can be found in [13]. We start with a very qualitative approach, which allows understanding the tube radiation phenomenon, and gives already a correct value for the real part of the input impedance at low frequencies. Indeed for a tube radiating into the infinite space, radiation is a particular case of discontinuities such as those studied in Chap. 7.

- Let us consider an abrupt change in cross section (Fig. 7.20): at low frequencies, the fluid can be regarded as incompressible (cf. Chap. 1, Sect. 1.5), thus there is flow rate conservation from one side of the discontinuity to the other side. If in addition the pressure is uniform in a straight cross section of each duct, the energy conservation yields

$$\Re e(Z_{\text{left}}) = \Re e(Z_{\text{right}}). \tag{12.119}$$

  (here the impedances are the acoustic impedances, i.e., a ratio pressure/flow rate). Close to the discontinuity, the pressure is not uniform, but if the straight cross sections are chosen at a certain distance of the discontinuity (i.e., one or two diameters), only the planar mode is present, and this expression is valid. Otherwise the discontinuity impedance Z_d is purely imaginary [see Eq. (7.158)], and the Expression (12.119) remains valid at the discontinuity. This is exactly what we need to match the internal and external fields.

If the tube on the right is infinite, the impedance to the right is: $\rho c/S_{\text{right}}$, and we have found a first expression of the real part of the radiation impedance Z_{left} of the left tube into an infinite tube. The reflection coefficient R_ℓ at the end of this tube is found to be:

$$|R_\ell|^2 = \frac{(R_R - 1)^2 + X_R^2}{(R_R + 1)^2 + X_R^2} \simeq \left(\frac{R_R - 1}{R_R + 1}\right)^2,$$

[14] This means $ka < 1.8$ [cf. Eq. (7.147)]. For a clarinet this gives $f < 14$ kHz, but for tapered instruments, the limit frequency can be much lower. The following equation can be used up to $ka = 3.8$ for the case of a perfect axisymmetry (see Chap. 7), but it is not the case of wind instruments, because of the exciter geometry and of the existence of toneholes.

if we denote $Z_{\text{right}} S_{\text{left}}/\rho c = R_R + jX_R$ (see Sect. 7.3.2 in Chap. 7). Indeed at low frequencies the effect X_R of the added mass tends to 0. Therefore, the larger the cross section discontinuity, the stronger the reflection.

- This reasoning can be extended to the case where the left tube is terminated in an infinite cone (with index b): there is a matching volume, as shown in Fig. 7.13, where pressure and velocity have complicated profiles, but, at low frequencies, the flow rate is conserved. The field can be expanded in the cone by using spherical Bessel functions. The fundamental mode is the mode with a spherical symmetry. Its characteristic admittance (ratio pressure/flow rate) is given by:

$$Y = \frac{S_b}{\rho c}\left[1 + \frac{1}{jkr_b}\right].$$

  [see Eq. (7.79)]. At low frequencies, this implies

$$\Re e(Z_{\text{right}}) = \frac{\rho c}{S_b}\frac{k^2 r_b^2}{1 + k^2 r_b^2} \tag{12.120}$$

$$\simeq \frac{\rho c}{S_b} k^2 r_b^2 = \frac{\rho c k^2}{2\pi(1 - \cos\theta_b)}. \tag{12.121}$$

  Here, θ_b is the apex semi-angle of the cone, because the impedance is defined on a spherical cap.[15] When the cone is opened up to become an infinite flange, θ_b tends to $\pi/2$, and the real part of the radiation impedance decreases down to:

$$\Re e(Z_R) = \frac{\rho c k^2}{2\pi}\,. \tag{12.122}$$

  The explanation of the decrease is intuitive, because the discontinuity increases, thus the reflection coefficient increases and the reflection tends to be total.
- The latter result can be obtained directly if we assume that the tube radiates with an infinite flange and that waves are spherical far enough from the tube end (Fig. 12.28). This assumption is confirmed by the fact that the result does not depend on the radius of the hemisphere. And for an unflanged tube (i.e., with a zero thickness) the surface where waves are spherical is a sphere,[16] and we obtain

$$\Re e(Z_R) = \frac{\rho c k^2}{4\pi}. \tag{12.123}$$

[15] Formula (12.121) is not valid for a cone with weak taper: when r_b tends to infinity, the impedance should tend to $\rho c/S_{\text{left}}$, which is the characteristic impedance of the cylindrical tube. In order to find this result, we must keep the expression (12.120) with $S_{\text{gauche}} = S_b$, because the matching volume tends to zero.

[16] In fact, we have here a complete sphere reduced by the external cross section of the tube. Nevertheless, because the radius is small compared to the wavelength, this reduction may be ignored.

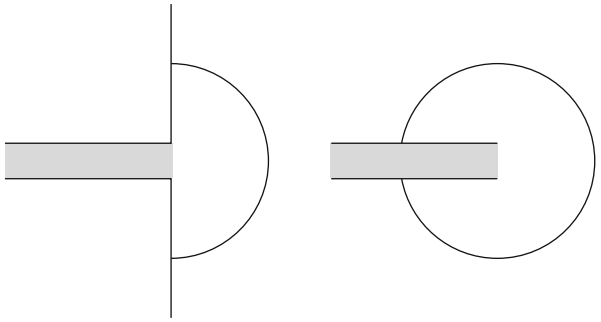

Fig. 12.28 Radiation of a tube with an infinite flange (*left*) and of an unflanged tube (*right*). The flow rate and power are conserved on a hemisphere and a quasi-complete sphere, respectively. The radius of the sphere is sufficiently large for waves to be spherical on it

Therefore the previous approach allows determining the real part of the radiation impedance at low frequencies. It is nothing but that of a monopole radiating into the infinite space expressed in (12.12). Incidentally we notice that, using the same argument, the radiation of a diverging conical tube produces a reflection smaller than the one of a cylinder. In what follows, the formulas are limited to cylindrical tubes, because there are no known formulas for a cone or a flared bell. As to the termination of a bell, i.e., the shape of the flange, plays a determinant role on radiation and, as one can imagine, there are no simple formulas for these cases. The matching of the field between the bell and the infinite space presents a difficulty of a nature similar to that of the field analysis inside the bell. The case of the Bessel horns (see Sect. 7.5.1 in Chap. 7) illustrates the fact that the separation between the tube and the flange is less relevant than for a cylinder.

12.6.1.2 Radiation Impedance of a Cylinder with an Infinite Flange

Now we wholly treat a rather simple case, that of a cylinder radiating with an infinite flange. It is somewhat academic but interesting, and it can be applied as a first approximation for a side hole, when the flange is the external surface of the tube. Then the two cases of a tube without flange and with a finite flange (which can be the tube thickness) are considered. In a cylinder, where the planar mode only propagates, evanescent modes can exist near the tube end, but they all are with a radial symmetry $n = 0$, which is the symmetry of the problem. The calculation of the radiation with an infinite flange is done thanks to the Rayleigh integral (12.98) together with the modal expansion given in Sect. 7.6.3.2 of Chap. 7. Pressure and velocity are expanded in duct modes (in a vector form), and a matrix radiation impedance $\mathbb{Z}_R$ is deduced for the modes with radial symmetry $\Phi_{i0}(r) = J_0(\gamma_{i0} r)$:

$$\boldsymbol{P} = \mathbb{Z}_R \boldsymbol{U} \quad \text{where} \quad Z_{ij} = \frac{j\omega\rho}{2\pi} \frac{1}{S^2} \int_S \int_S \boldsymbol{\Phi}_{i0}(r) \Phi_{j0}(r') \frac{\exp(-jk\,|r - r'|)}{|r - r'|} dS\, dS'. \tag{12.124}$$

Similarly to the method used for a cross section discontinuity, it remains to separate the planar mode (p, u) from the higher order modes $(\boldsymbol{P}', \boldsymbol{U}')$, then to close the latter on their characteristic impedance $(\boldsymbol{P}' = -\mathbb{Z}'\boldsymbol{U}')$, because the tube end is assumed to be far from any other discontinuity. Using evident notations, we write

$$\begin{pmatrix} p \\ \boldsymbol{P}' \end{pmatrix} = \begin{pmatrix} Z_{R00} & {}^t\boldsymbol{z} \\ \boldsymbol{z} & \mathbb{Z}'_R \end{pmatrix} \begin{pmatrix} u \\ \boldsymbol{U}' \end{pmatrix},$$

where

$$p = Z_R u, \text{ with } Z_R = Z_{R00} - {}^t\boldsymbol{z}(\mathbb{Z}'_R + \mathbb{Z}')^{-1}\boldsymbol{z}. \tag{12.125}$$

In this expression the quantity Z_{R00} is the plane piston approximation, which was discussed in Sect. 7.6.3.2 of Chap. 7, and is often used since Rayleigh. This author calculated the ratio of the averaged pressure to the piston velocity starting from formula (12.98), and obtained a formula where modified Bessel functions, called Struve functions, intervene. The low-frequency approximation is the following:

$$Z_{R00} = \frac{\rho c}{S}\left[\frac{1}{2}(ka)^2 + j\frac{8}{3\pi}ka\right] + O\left[(ka)^3\right]. \tag{12.126}$$

The imaginary part corresponds to a length correction of $\Delta\ell = 8a/(3\pi) = 0.85a$ (cf. the analysis of Chap. 4, Sect. 4.6.4), and the real part is that given by Eq. (12.122).

For a tube, several authors made the computation (see, for example, [23]). At low frequencies, the result is very close to that of the plane piston, but the length correction is $\Delta\ell = 0.8216a$, as calculated by Rayleigh himself. At other frequencies, the impedance can be written with respect to the complex reflection coefficient R_ℓ:

$$Z_R = \frac{\rho c}{S}\frac{1 + R_\ell}{1 - R_\ell} = j\frac{\rho c}{S}\tan\left[k\Delta\ell + \frac{j}{2}\ln|R_\ell|\right] \tag{12.127}$$

$$\text{where} \quad R_\ell = -|R_\ell|\exp(-2jk\Delta\ell) \tag{12.128}$$

[cf. Eq. (4.43)]. As a consequence, both the length correction $\Delta\ell$ and the modulus of the reflection coefficient depend on frequency. Figure 12.29 shows the two results (the exact formula and the plane piston approximation). The behaviors are different at lower and higher frequencies, with a transition around $ka = 1$ or 2. At higher frequencies, the real part tends to the characteristic impedance, the imaginary part tends to 0, and the length correction decreases significantly.

An approximate formula was recently obtained [17, 30], by seeking an expansion ensuring the following properties:

- symmetry $Z(\omega) = Z^*(-\omega)$;
- causality of the reflection function (and of the inverse FT of the impedance);

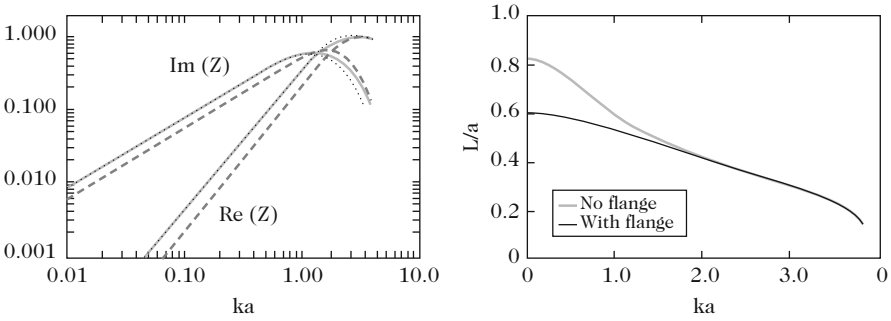

Fig. 12.29 *Left plot*: real and imaginary parts of the radiation impedance for a tube without flange (*gray dashed line*), with an infinite flange (*gray solid line*) and with an infinite flange in the approximation of the plane piston (*dotted line*). At higher frequencies, the real part tends to the characteristic impedance while the imaginary part tends to 0. *Right plot*: length correction $\Delta\ell$ with respect to frequency: with an infinite flange (*gray line*) and without flange (*black line*)

- a correct behavior of Z_R at low frequencies, with the following notation: $Z_R = Z_c\left[j\delta ka + \frac{1}{2}\beta(ka)^2\right]$;
- convergence of Z_R to the characteristic impedance at higher frequencies.

This formula is written as follows:

$$R_\ell = -\frac{1 + n_1 jka}{1 + d_1 jka + d_2(jka)^2}\ , \text{where} \tag{12.129}$$

$$n_1 = 0.182;\ d_1 = 2\delta + n_1 = 1.825\ ;\ d_2 = \frac{1}{2}\left(d_1^2 - n_1^2\right) - 2\beta = 0.649 \tag{12.130}$$

$$\delta = 0.8236;\ \beta = \frac{1}{2}. \tag{12.131}$$

The inverse FT of $R_\ell(\omega)$ can be deduced: for $t > 0$, it is the superposition of two real decreasing exponentials, because the poles of the polynomial $1 + d_1 x + d_2 x^2$ are real. The corresponding formula for the impedance is

$$Z_R = Z_c \frac{j\delta ka + \frac{1}{2}d_2(jka)^2}{1 + \frac{1}{2}(n_1 + d_1)jka + \frac{1}{2}d_2(jka)^2}. \tag{12.132}$$

12.6.1.3 Radiation Impedance of an Unflanged Tube

The calculation for an unflanged tube is significantly more complicated. It was done by using the analytic continuation in the complex plane (i.e., the Wiener–Hopf method) by Levine and Schwinger [18]. At low frequencies the result is the following:

$$Z_R = \frac{\rho c}{S}\left[\frac{1}{4}(ka)^2 + 0.6133jka\right]. \tag{12.133}$$

The real part is that given by Eq. (12.123), and the imaginary part corresponds to a length correction of $\Delta\ell = 0.6133a$. Figure 12.29 shows the comparison between this result, which is probably the most useful, with that of the previous cases. The approximate formula (12.129) can be used, with:

$$n_1 = 0.167\,;\, d_1 = 2\delta + n_1 = 1.393\,;\, d_2 = \frac{1}{2}\left(d_1^2 - n_1^2\right) - 2\beta = 0.457 \tag{12.134}$$

$$\delta = 0.6133;\ \beta = \frac{1}{4}. \tag{12.135}$$

12.6.1.4 Radiation Impedance of a Tube with a Finite Flange

The two above presented cases are extreme cases. Calculations were done for the case of a tube with a finite flange. The external diameter is denoted $2b$. Fit formulas were obtained for the reflection coefficient, based upon experimental and numerical results [7]:

$$R_\ell = R_\ell^* - 0.43\frac{a(b-a)}{b^2}\sin^2\left[\frac{kb}{1.85 - a/b}\right]e^{-jkb\left[1+a/b\left(2.3-a/b-0.3(ka)^2\right)\right]}\,; \tag{12.136}$$

$$R_\ell^* = -e^{-2jk\Delta\ell^*} \quad \Delta\ell^* = \Delta\ell_\infty^* + \frac{a}{b}(\Delta\ell_0^* - \Delta\ell_\infty^*) + 0.057\frac{a}{b}\left[1 - \left(\frac{a}{b}\right)^5\right]a. \tag{12.137}$$

The quantities $\Delta\ell_0^*$ and $\Delta\ell_\infty^*$ are complex length corrections (the indices 0 and ∞ correspond to the cases without flange and with infinite flange, respectively), and are deduced from formulas (12.129) to (12.135) by:

$$k\Delta\ell^* = k\Delta\ell + \frac{j}{2}\ln|R_\ell|\,.$$

In formula (12.136), the function $\sin^2$ evidences oscillations which are due to reflections on the external edges of the tube. Other geometrical shapes or other terminations were studied by some authors [7, 12, 24, 29]: as it was above mentioned, the issue is complicated and cannot be clearly distinguished from that of the extension of a tube into a small bell. Concerning the radiation by bells, the case of a conical horn has been treated above. If the plane wave approximation is accepted, it is consistent to choose the radiation impedance of a cylindrical tube. However, the frequency limit of validity is rather low, similarly to that of the horn

equation (cf. Sect. 7.6.3.5, Chap. 7). In order to study this matter in a more precise way, numerical methods need to be used, such as the Boundary Element Method (cf. Sect. 12.5.3.6), or experiments can be carried out.

12.6.1.5 Radiation Impedance of a Tonehole

The radiation by a tonehole is another rather complicated problem. When the radius tends to 0, the radiation is expected to become similar to that with an infinite flange, and the corresponding formula is in general satisfactory. However, holes are often provided with keys which are perforated or not and modify the radiation: some indications can be found on their effect, in particular in Refs. [9, 22].

12.6.2 Field Radiated by a Tube: Directivity

For an unflanged tube Levine and Schwinger [18] gave an approximated formula for the far field. It can be written in the following form (if $\theta = 0$ in the tube axis):

$$P(r,\theta) = j\omega\rho U_\ell \; D(\theta) \; F(\theta) \; \frac{e^{-jkr}}{4\pi r} \quad \text{where}$$
$$D(\theta) = \frac{2J_1(ka\sin\theta)}{ka\sin\theta} \quad \text{and } F(\theta) = 1 + \frac{Z_R S}{\rho c}\cos\theta. \tag{12.138}$$

At the lowest frequencies the radiation is that of a monopole. The directivity factor $D(\theta)$ is that for a plane piston in an infinite baffle.

The factor $F(\theta)$, can be interpreted as the result of the superposition of a plane piston in an infinite baffle and an unflanged piston, which behaves as a dipole with the directivity factor $D(\theta)\cos\theta$: it can be shown that this superposition corresponds to a piston radiating without flange from one side only[17] [5]. The existence of this dipole makes the radiation forwardly and rearwardly very asymmetrical (notice that the result $|F(\pi)|\,/\,|F(0)| = |R_\ell|$ is exact). At higher frequencies, the factor $F(\theta)$ tends to $(1+\cos\theta)$, which is the directivity of a cardioid.

Figure 12.30 shows the directivity of a tube for different values of ka, and a comparison with the case of a plane piston in an infinite baffle. The maximum is obtained for $\theta = 0°$, and the minimum near $\theta = 130°$. For example, for $ka = 1$, with respect to $\theta = 0°$, it is found -2.7 dB for $\theta = 90°$, -3.5 dB for $\theta = 131°$, and -3.3 dB for $\theta = 180°$. At higher frequencies, the formula (12.138) diverges from the exact value, except for 0° and 180°.

[17] For this case the imaginary part is found to be $2R/\pi = 0.6366R$, and is slightly larger than that of a unflanged tube: this difference can be compared to that between a tube and a plane piston.

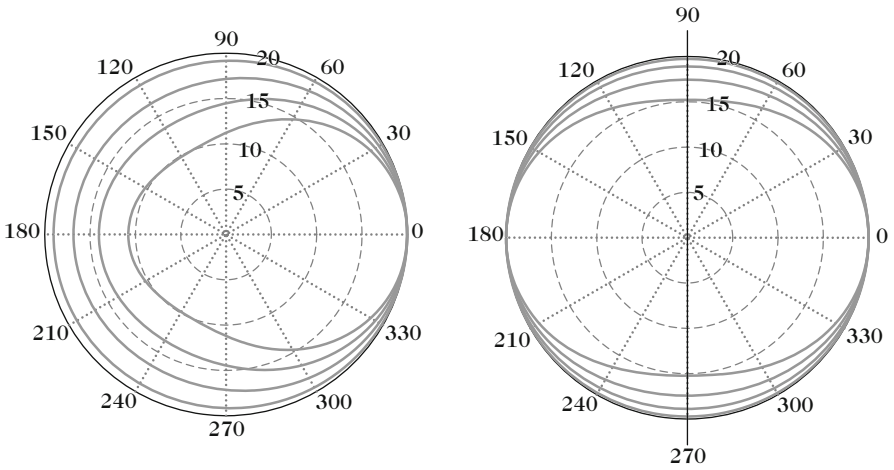

Fig. 12.30 Directivity, in decibels, of an unflanged tube (*left plot*), $D(\theta)F(\theta)$, and of a plane piston in an infinite baffle, $D(\theta)$ (*right plot*). The values of the frequency are, from the outside to the inside: $ka = 0.5; 1; 1,5; 2$

Considering now the argument of the function $F(\theta)$, we see that, for small ka, it is equal to $k\Delta\ell \cos\theta$. A geometrical reasoning shows that the acoustic center of the waves produced by the tube is located at the distance $\Delta\ell$ from the tube end: therefore the length correction is also a quantity related to the radiated field.

Finally, Ando [1] showed that the directivity is slightly modified when the tube thickness is taken into account, and that the acoustic center is no longer located exactly at a distance equal to the length correction of the tube.

For a bell, experiment shows that the directivity globally increases at higher frequencies, and is similar to that of a cylinder. Figure 12.31 shows experimental results, which are obtained by exciting a trombone with a loudspeaker at its input (the real radiation can be slightly different because of the mean flow). However, as the opening is wide, the directivity of the bell is significant even at rather low audible frequencies. This result was confirmed by Martin, who made similar measurements [19]. Such a phenomenon is very well known by the players, who modify the orientation of their instrument in order to adjust the perception of higher frequencies by the listeners.

12.6.3 Radiation by Two Tubes or Two Orifices

When two sources are close together, they have a mutual influence. From the integral formulation of type (12.61), we can calculate the average pressure on two surfaces with respect to the flow rate of each of them, and the result can be written in the general form of a radiation impedance matrix (or an admittance matrix):

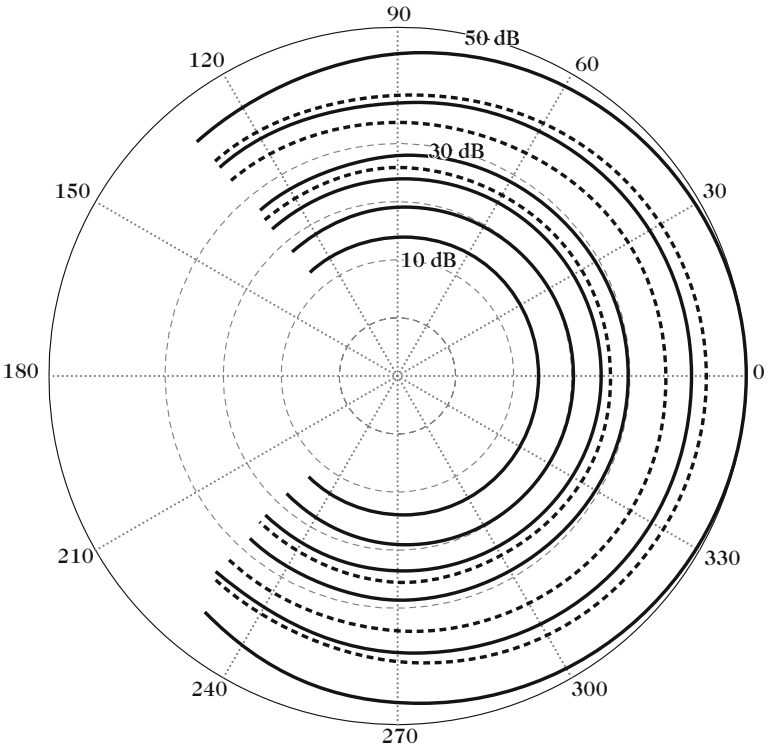

Fig. 12.31 Radiation of a trombone with closed slide excited by a loudspeaker. The directivity is measured for different harmonics of the note. The corresponding frequencies are 113; 171; 229; 294; 346; 406; 465; 521; 590 Hz. The increase from the lower frequencies to the higher ones is plotted from the inside to the outside. It can be noticed that the directivity increases with frequency. (Courtesy of R. Caussé)

$$P_1 = Z_{11}U_1 + Z_{12}U_2$$
$$P_2 = Z_{21}U_1 + Z_{22}U_2. \tag{12.139}$$

Z_{11} and Z_{22} are "self-impedances," and $Z_{12} = Z_{21}$ are mutual impedance, which are equal because of reciprocity. It can be useful to know them when the ends of two tubes are close together, or when two orifices of a tube are close together, as it is the case for open toneholes. We examine this issue in detail at lower frequencies, and focus on the power balance. A simple approximate formula can be deduced, together with a validity condition.

The mutual impedances generally are as difficult to calculate as the self-impedances, which were calculated in the previous section. The literature on this subject is wide. As an example, we can start with two pistons located in the same infinite baffle. The formula of the mutual impedances can be then directly deduced from the Rayleigh integral (12.98):

$$Z_{12} = Z_{21} = j\rho c \frac{k}{2\pi} \frac{1}{S_1 S_2} \int_{S_1} \int_{S_2} \frac{e^{-jk|\boldsymbol{r}_1 - \boldsymbol{r}_2|}}{|\boldsymbol{r}_1 - \boldsymbol{r}_2|} dS_1 dS_2. \tag{12.140}$$

We consider two elementary sources, separated by a distance d. A series expansion can be calculated if the quantity $k\,[d + (a_1 + a_2)/2]$ is assumed to be small [25]. We limit the calculation to the real part, which is the only term involved in the power balance. The result is

$$\Re e(Z_{ii}) = \rho c \frac{k^2}{2\pi} \left[1 - \frac{k^2 a_i^2}{6} + O(k^4 a_i^4) \right], \; i = 1, 2\,; \tag{12.141}$$

$$\Re e(Z_{12}) = \rho c \frac{k^2}{2\pi} \left[1 - \frac{1}{6} k^2 \left(d^2 + \frac{a_1^2 + a_2^2}{2} \right) + O\left(k^4 d^4, k^4 a_1^4, k^4 a_2^4\right) \right]. \tag{12.142}$$

The power averaged over a period is written in the following form:

$$\mathscr{P} = \frac{1}{2} \Re e(p_1 U_1^*) + \frac{1}{2} \Re e(p_2 U_2^*) \;\text{ or} \tag{12.143}$$

$$\begin{aligned} \mathscr{P} = {} & \frac{1}{2} |U_1|^2 \Re e(Z_{11} - Z_{12}) \\ & + \frac{1}{2} |U_2|^2 \Re e(Z_{22} - Z_{12}) + \frac{1}{2} |U_1 + U_2|^2 \Re e(Z_{12}). \end{aligned} \tag{12.144}$$

For the case of the two pistons, we derive

$$\begin{aligned} \mathscr{P} = {} & \rho c \frac{k^2}{4\pi} |U_1 + U_2|^2 + \rho c \frac{k^4}{24\pi} |U_1|^2 \left(\frac{a_2^2 - a_1^2}{2} + d^2 \right) \\ & + \rho c \frac{k^4}{24\pi} \left[|U_2|^2 \left(\frac{a_1^2 - a_2^2}{2} + d^2 \right) \right. \\ & \left. - |U_1 + U_2|^2 \left(\frac{a_1^2 + a_2^2}{2} + d^2 \right) \right]. \end{aligned} \tag{12.145}$$

For point sources, it can be checked that the result is the same than Eq. (12.28) by a factor of two, since the pistons here radiate into a half-space.

Formula (12.145) shows that at low frequencies the radiation is that of a monopole with flow rate $|U_1 + U_2|^2$, which is proportional to ω^2, but if the two sources have the same amplitude and are opposite in phase, the radiation is that of a dipole, proportional to ω^4. This kind of analysis allows understanding why a vented box loudspeaker[18] paradoxically radiates as a dipole at lower frequencies

[18]The enclosure partially separates the rear face of a loudspeaker; it has several openings, contrary to a closed box loudspeaker.

and as a monopole at higher frequencies, because the two sources are linked by a relationship of kind: $U_1 = U_2(\omega^2/\omega_r^2 - 1)$, where ω_r is the Helmholtz angular resonance frequency of the enclosure. A similar case is that of stringed instruments with openings: this was analyzed in connection with the sound hole sum rule in Eq. (12.86).

For two tubes radiating in the same plane and without flange, the approximation of the plane piston can be used [16]. By applying again the superposition principle, we obtain for the real part of the mutual impedance the Expression (12.142), divided by a factor 2. This analysis could be extended, but it is rather academic, because the two tube ends rarely are in the same plane. This result can be used, for instance for toneholes, but we can simply use the approximation, and more generally the formula of a monopole radiation:

$$Z_{12} = j\rho c \frac{k}{4\pi} \frac{e^{-jkd}}{d}. \tag{12.146}$$

In summary, the previous analysis allows understanding, at least for a particular case, under which condition this condition is valid: the distance d needs to be large compared to the source radii. This very simplified expression will be used in order to analyze the radiation of complex sources in Chap. 14.

References

1. Ando, Y.: On the sound radiation from semi-infinite circular pipe of certain wall thickness. Acustica **22**, 219–225 (1969–1970)
2. Arfken, G., Weber, H.J.: Mathematical Methods for Physicists. Elsevier, Amsterdam (2005)
3. Brooke, M.: Numerical simulation of guitar radiation fields using the boundary element method. Ph.D. thesis, University of Wales, College of Cardiff (1992)
4. Chaigne, A.: The song of wine glasses (in French). Sci. et Avenir **100**, 52–57 (1995)
5. Crane, P.: Method for the calculation of the acoustic radiation impedance of unbaffled and partially baffled piston source. J. Sound Vib. **5**, 255–277 (1967)
6. Da Silva, A., Scavone, G.: Lattice Boltzmann simulations of the acoustic radiation from waveguides. J. Phys. A Math. Theor. **40**, 397–408, et 9721 (2007)
7. Dalmont, J.P., Nederveen, K., Joly, N.: Radiation impedance of tubes with different flanges: numerical and experimental investigation. J. Sound Vib. **244**(3), 505–534 (2001)
8. Dérogis, P.: Analysis of the vibrations and radiation of an upright piano soundboard, and design of a system for reproducing its acoustic field (in French). Ph.D. thesis, Université du Maine, Le Mans (1997)
9. Dickens, P.: Flute acoustics: measurement, modelling and design. Ph.D. thesis, University of New South Wales, Australia (2007)
10. Fahy, F.: Foundations of Engineering Acoustics. Academic, London (2000)
11. French, A.P.: In vino veritas: a study of wineglass acoustics. Am. J. Phys. **51**, 688–694 (1983)
12. Hélie, T., Rodet, X.: Radiation of a pulsating portion of a sphere: application to horn radiation. Acta Acustica United with Acustica **89**, 565–577 (2003)
13. Hocter, S.: Sound radiated from a cylindrical duct with Keller's geometrical theory. J. Sound Vib. **231**, 1243–1256 (2000)

14. Jacobsen, F., Juhl, P.: Radiation of sound. Acoustic Technology, Technical University of Denmark (2006)
15. Junger, M.C.: Sound radiation by resonances of free-free beams. J. Acoust. Soc. Am. **52**, 332–334 (1972)
16. Kergomard, J.: On the response of a vented box loudspeaker system at very low frequencies. In: 75th Convention of the Audio Engineering Society (preprint 2060), Paris (1984)
17. Kergomard, J., Lefebre, A., Scavone, G.: Matching of fundamental modes at a junction of a cylinder and a truncated cone; application to the calculation of some radiation impedances. Acta Acustica United with Acustica **101**, 1189–1198 (2015)
18. Levine, H., Schwinger, J.: On the radiation of sound from an unflanged circular pipe. Phys. Rev. **73**, 383–406 (1948)
19. Martin, D.W.: Directivity and the acoustic spectra of brass wind instruments. J. Acoust. Soc. Am. **13**(3), 309–313 (1942)
20. Morse, P.M., Ingard, K.: Theoretical Acoustics. McGraw Hill, New York (1968)
21. Munt, R.: Acoustic radiation from a circular cylinder in a subsonic stream. J. Inst. Math. Appl. **16**, 1–10 (1975)
22. Nederveen, C.J.: Acoustical Aspects of Woodwind Instruments. Northern Illinois University Press, Illinois. New edition, 1998 (1969)
23. Norris, A., Sheng, I.: Acoustic radiation from a circular pipe with an infinite flange. J. Sound Vib. **135**, 85–93 (1989)
24. Peters, M., Hirschberg, A., Reijnen, A., Wijnands, A.: Damping and reflection coefficient measurements for an open pipe at low mach and low Helmholtz numbers. J. Fluid Mech. **256**, 499–534 (1993)
25. Pritchard, R.: Mutual acoustic impedance between radiators in an infinite rigid plane. J. Acoust. Soc. Am. **32**, 730–737 (1960)
26. Rienstra, S., Hirschberg, A.: An Introduction to Acoustics. Eindhoven University of Technology, Eindhoven (2006)
27. Rossing, T.D.: Acoustics of the glass harmonica. J. Acoust. Soc. Am. **95**, 1106–1111 (1994)
28. Russel, D.A.: On the sound field radiated by a tuning fork. Am. J. Phys. **68**(12), 1139–1145 (2000)
29. Selamet, A., Ji, Z.L., Kach, R.A.: Wave reflections from duct terminations. J. Acoust. Soc. Am. **109**(4), 1304–1311 (2001)
30. Silva, F., Kergomard, J., Norris, A., Mallaroni, B.: Approximation formulae for the acoustic radiation impedance of a cylindrical pipe. J. Sound Vib. **322**, 255–263 (2009)
31. Temkin, S.: Elements of Acoustics. Acoustical Society of America, Melville (2001)
32. von Estorff, O. (ed.): Boundary Elements in Acoustics: Advances and Applications. WIT Press, Southampton (2000)
33. Weinreich, G.: Sound hole sum rule and the dipole moment of the violin. J. Acoust. Soc. Am. **77**(2), 710–718 (1985)
34. Weinreich, G., Arnold, E.B.: Method for measuring acoustic radiation fields. J. Acoust. Soc. Am. **68**(2), 404–411 (1980)
35. Williams, E.G.: Fourier Acoustics: Sound Radiation and NearField Acoustical Holography. Academic, New York (1999)
36. Wu, T.W. (ed.): Boundary Element Acoustics: Fundamentals and Computer Codes. WIT Press, Southampton (2000)